

R E V I E W   A R T I C L E

## Metal-insulator transition in two-dimensional electron systems

S V Kravchenko

Physics Department, Northeastern University, Boston, MA 02115, USA

M P Sarachik

Physics Department, City College of the City University of New York, New York, NY 10031, USA

**A b s t r a c t .** The interplay between strong Coulomb interactions and randomness has been a long-standing problem in condensed matter physics. According to the scaling theory of localization, in two-dimensional systems of noninteracting or weakly interacting electrons, the ever-present randomness causes the resistance to rise as the temperature is decreased, leading to an insulating ground state. However, new evidence has emerged within the past decade indicating a transition from insulating to metallic phase in two-dimensional systems of strongly interacting electrons. We review earlier experiments that demonstrate the unexpected presence of a metallic phase in two dimensions, and present an overview of recent experiments with emphasis on the anomalous magnetic properties that have been observed in the vicinity of the transition.

E-mail: s.kravchenko@neu.edu; sarachik@sci.ccny.cuny.edu

Journal ref.: Rep. Prog. Phys. 67, 1 (2004)

Metal-insulator transition in 2D	2
1 INTRODUCTION	3
2 EXPERIMENTAL RESULTS IN ZERO MAGNETIC FIELD	5
2.1 Resistance in zero magnetic field, experimental scaling, reflection symmetry . . . . .	5
2.2 How universal is $\rho(T)$ ? . . . . .	7
2.3 Critical density . . . . .	12
2.4 Does weak localization survive in the presence of strong interactions? .	15
3 THE EFFECT OF A MAGNETIC FIELD	18
3.1 Resistance in a parallel magnetic field . . . . .	18
3.2 Scaling of the magnetoresistance; evidence for a phase transition . . .	22
4 SPIN SUSCEPTIBILITY NEAR THE METAL-INSULATOR TRANSITION	26
4.1 Experimental measurements of the spin susceptibility . . . . .	26
4.2 Effective mass and g-factor . . . . .	31
4.3 Electron-electron interactions near the transition . . . . .	34
5 HOW DOES ALL THIS FIT THEORY?	35
5.1 The diffusive regime: Renormalization group analysis . . . . .	36
5.2 Farther from the transition (the ballistic regime) . . . . .	39
5.3 Approaches not based on Fermi liquid . . . . .	42
6 CONCLUSIONS	43
7 REFERENCES	45

## 1. INTRODUCTION

In two-dimensional electron systems, the electrons are confined to move in a plane in the presence of a random potential. According to the scaling theory of localization (Abraham et al 1979), these systems lie on the boundary between high and low dimensions insofar as the metal-insulator transition is concerned. The carriers are always strongly localized in one dimension, while in three dimensions, the electronic states can be either localized or extended. In the case of two dimensions the electrons may conduct well at room temperature, but a weak logarithmic increase of the resistance is expected as the temperature is reduced. This is due to the fact that, when scattered from impurities back to their starting point, electron waves interfere constructively with their time reversed paths. While this effect is weak at high temperatures due to inelastic scattering events, quantum interference becomes increasingly important as the temperature is reduced and leads to localization of the electrons, albeit on a large length scale; this is generally referred to as "weak localization". Indeed, thin metallic films and two-dimensional electron systems fabricated on semiconductor surfaces were found to display the predicted logarithmic increase of resistivity (Dolan and Oshero 1979; Bishop et al 1980, 1982; Uren et al 1980), providing support for the weak localization theory.

The scaling theory does not explicitly consider the effect of the Coulomb interaction between electrons. The strength of the interactions is usually characterized by the dimensionless Wigner-Seitz radius,  $r_s = 1/(n_s)^{1/2} a_B$  (here  $n_s$  is the electron density and  $a_B$  is the Bohr radius in a semiconductor). In the experiments mentioned above, the Coulomb interactions are relatively weak. Indeed, these experiments are in agreement with theoretical predictions (Altshuler, Aronov and Lee 1980) that weak electron-electron interactions ( $r_s \ll 1$ ) increase the localization even further. As the density of electrons is reduced, however, the Wigner-Seitz radius grows and the interactions provide the dominant energy of the system. No analytical theory has been developed to date in the strongly-interacting limit ( $r_s \gg 1$ ). Finkelstein (1983, 1984) and Castellani et al (1984) predicted that for weak disorder and sufficiently strong interactions, a 2D system should scale towards a conducting state as the temperature is lowered. However, the scaling procedure leads to an increase in the effective strength of the interactions and to a divergent spin susceptibility, so that the perturbative approach breaks down as the temperature is reduced toward zero. Therefore, the possibility of a 2D metallic ground state stabilized by strong electron-electron interactions was not seriously considered.

Recent progress in semiconductor technology has enabled the fabrication of high quality 2D samples with very low randomness in which measurements can be made at very low carrier densities. The strongly-interacting regime ( $r_s \gg 1$ ) has thus become experimentally accessible. Experiments on low-disordered 2D silicon samples (Kravchenko et al 1994, 1995, 1996) demonstrated that there are surprising and dramatic differences between the behaviour of strongly interacting systems at  $r_s > 10$  as compared with weakly-interacting systems: with increasing electron density, one can cross from the regime where the resistance diverges with decreasing temperature (insulating behaviour) to a regime where the resistance decreases strongly with decreasing  $T$  (metallic behaviour). These results were met with great scepticism and largely overlooked until 1997, when they were confirmed in silicon MOSFETs from a different source (Popovic et al 1997) and in other strongly-interacting 2D systems (Coleridge et al 1997; Hanein et al 1998a; Papadakis and Shayegan 1998). Moreover, it

was found (Simonian et al 1997b; Pudalov et al 1997; Simmons et al 1998) that in the strongly-interacting regime, an external magnetic field strong enough to polarize the electrons' spins induces a giant positive in-plane magnetoresistance and completely suppresses the metallic behaviour, thus implying that the spin state is central to the high conductance of the metallic state. This finding was in qualitative agreement with the prediction of Finkelstein and Castellani et al that for spin-polarized electrons, only an insulating ground state is possible in a disordered 2D system even in the presence of strong interactions. Subsequent experiments (Okamoto et al 1999; Kravchenko et al 2000b; Shashkin et al 2001, 2002; Vitkalov et al 2001b, 2002; Pudalov et al 2002b; Zhu et al 2003) have shown that there is a sharp enhancement of the spin susceptibility as the metal-insulator transition is approached; indications exist that in silicon MOSFETs, the spin susceptibility may actually diverge at some sample-independent electron density  $n \approx 8 \times 10^{10} \text{ cm}^{-2}$ .

In silicon samples with very low disorder potential, the critical density for the metal-insulator transition was found to be at or very near  $n_c$  (Shashkin et al 2001a, 2002; Vitkalov et al 2001b, 2002), indicating that the metal-insulator transition observed in these samples is a property of a clean disorder-free 2D system, rather than being a disorder-driven transition. In such samples, the metallic and insulating regimes are divided by a temperature-independent separatrix with  $3h = e^2$ , in the vicinity of which the resistivity displays virtually universal critical behaviour. However, in samples with relatively strong disorder, the electrons become localized at densities significantly higher than  $n_c$ : from  $1.44 \times 10^{10}$  to  $6.6 \times 10^{10} \text{ cm}^{-2}$  (Prus et al 2002), and even as high as  $1.6 \times 10^{10} \text{ cm}^{-2}$  (Pudalov et al 1999), indicating that the localization transition in these samples is driven by disorder.

We suggest that there has been a great deal of confusion and controversy caused by the fact that often no distinction has been made between results obtained in systems with relatively high disorder and those obtained for very clean samples, and also because in many experimental studies, a change in the sign of the derivative  $dR/dT$  has always been assumed to signal a metal-insulator transition. In this review, we focus our attention on results for very clean samples.

The experimental findings described above were quite unexpected. Once accepted, they elicited strong and widespread interest among theorists, with proposed explanations that included unusual superconductivity (Phillips et al 1998), charging/discharging of contaminations in the oxide (Altshuler and Maslov 1999), the formation of a disordered Wigner solid (Chakravarty et al 1999), inter-subband scattering (Yaish et al 2000) and many more (for a review, see Abrahamson, Kravchenko and Sarachik 2001). It is now well-documented that the metallic behaviour in zero magnetic field is caused by the delocalizing effect associated with strong electron-electron interactions which overpower quantum localization. In the "ballistic regime" deep in the metallic state, the conductivity is linear with temperature and derives from coherent scattering of electrons by Friedel oscillations (Zala, Narozhny and Leiner 2001). Closer to the transition, in the "diffusive" regime, the temperature dependence of the resistance is well described by a renormalization group analysis of the interplay of strong interactions and disorder (Punnoose and Finkelstein 2002). Within both theories (which consider essentially two limits of the same physical process) an external magnetic field quenches the delocalizing effect of interactions by aligning the spins,

<sup>z</sup> The fact that the parallel magnetic field promotes insulating behaviour in strongly interacting 2D systems was first noticed by Dolgoplov et al (1992).

and causes a giant positive magnetoresistance. However, the metal-insulator transition itself, as well as the dramatic increase of the spin susceptibility and effective mass in its close vicinity, still lack adequate theoretical description; in this region the system appears to behave well beyond a weakly interacting Fermi liquid.

In the next three sections, we describe the main experimental results that demonstrate the unexpected presence of a metallic phase in 2D and present an overview of recent experiments with emphasis on the anomalous magnetic properties observed in the vicinity of the metal-insulator transition.

## 2. EXPERIMENTAL RESULTS IN ZERO MAGNETIC FIELD

### 2.1. Resistance in zero magnetic field, experimental scaling, reflection symmetry

The first experiments that demonstrated the unusual temperature dependence of the resistivity (Kravchenko et al 1994, 1995, 1996) were performed on low-disordered silicon metal-oxide-semiconductor field-effect transistors (MOSFETs) with maximum electron mobilities reaching more than  $4 \times 10^4 \text{ cm}^2/\text{Vs}$ , mobilities that were considerably higher than in samples used in earlier investigations. It was the very high quality of the samples that allowed access to the physics at electron densities below  $10^{11} \text{ cm}^{-2}$ . At these low densities, the Coulomb energy,  $E_C$ , is the dominant parameter. Estimates for Si MOSFETs at  $n_s = 10^{11} \text{ cm}^{-2}$  yield  $E_C \approx 10 \text{ meV}$ , while the Fermi energy,  $E_F$ , is about  $0.6 \text{ meV}$  (a valley degeneracy of two is taken into account when calculating the Fermi energy, and the effective mass is assumed to be equal to the band mass,  $m_b$ .) The ratio between the Coulomb and Fermi energies,  $r = E_C/E_F$ , thus assumes values above 10 in these samples.

Figure 1 (a) shows the temperature dependence of the resistivity measured in units of  $h/e^2$  of a high-mobility MOSFET for 30 different electron densities  $n_s$  varying from  $7.12 \times 10^{10}$  to  $13.7 \times 10^{10} \text{ cm}^{-2}$ . If the resistivity at high temperatures exceeds the quantum resistance  $h/e^2$  (the curves above the dashed red line),  $\rho(T)$  increases monotonically as the temperature decreases, behaviour that is characteristic of an insulator. However, for  $n_s$  above a certain "critical" value,  $n_c$  (the curves below the "critical" curve that extrapolates to  $3h/e^2$  denoted in red), the temperature dependence of  $\rho(T)$  becomes non-monotonic: with decreasing temperature, the resistivity first increases (at  $T > 2 \text{ K}$ ) and then starts to decrease. At yet higher density  $n_s$ , the resistivity is almost constant at  $T > 4 \text{ K}$  but drops by an order of magnitude at lower temperatures, showing strongly metallic behaviour as  $T \rightarrow 0$ .

A striking feature of the  $\rho(T)$  curves shown in Figure 1 (a) for different  $n_s$  is that they can be made to overlap by applying a (density-dependent) scale factor along the  $T$ -axis. Thus, the resistivity can be expressed as a function of  $T=T_0$  with  $T_0$  depending only on  $n_s$ . This was demonstrated for several samples over a rather wide range of electron densities (typically  $(n_c - 2.5 \times 10^{10}) < n_s < (n_c + 2.5 \times 10^{10} \text{ cm}^{-2})$ ) and in the temperature interval 0.2 to 2 K. The results of this scaling are shown in Fig. 1 (b), where  $\rho$  is plotted as a function of  $T=T_0$ . One can see that the data collapse onto two separate branches, the upper one for the insulating side of the transition and the lower one for the metallic side. The thickness of the lines is largely governed by the noise within a given data set, attesting to the high quality of the scaling.

The procedure used to bring about the collapse and determine  $T_0$  for each  $n_s$  was the following. No power law dependence was assumed a priori for  $T_0$  versus  $(n_s - n_c)$ ; instead, the  $\rho(T)$  curves were successively scaled along the  $T$ -axis to coincide: the

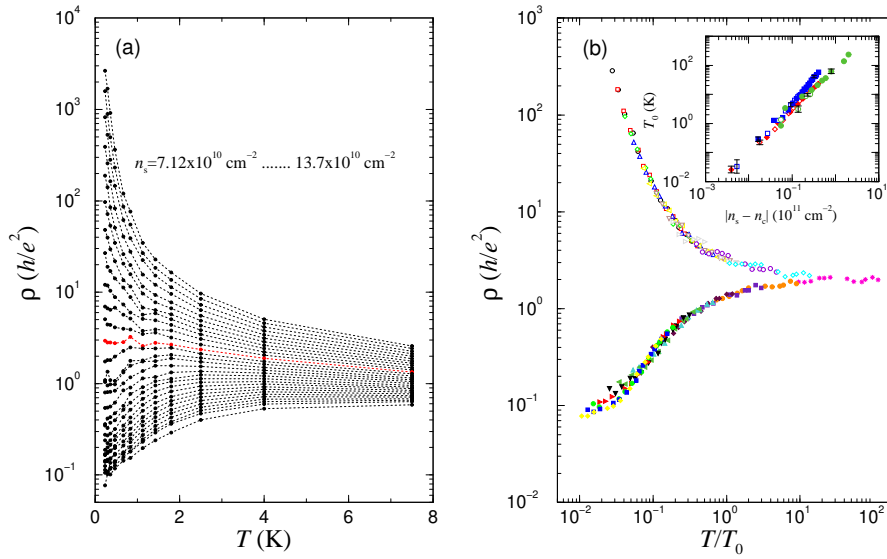


Figure 1. (a): temperature dependence of the  $B = 0$  resistivity in a dilute low-disordered Si MOSFET for 30 different electron densities  $n_s$  ranging from  $7.12$  to  $13.7 \cdot 10^{10} \text{ cm}^{-2}$ . (b): resistivity versus  $T = T_0$ , with  $T_0(n_s)$  chosen to yield scaling with temperature. The inset shows the scaling parameter,  $T_0$ , versus the deviation from the critical point,  $|n_s - n_c|$ ; data are shown for silicon MOSFETs obtained from three different wafers. Open symbols correspond to the insulating side and closed symbols to the metallic side of the transition. From Kravchenko et al (1995).

second "insulating" curve from the top was scaled along the  $T$ -axis to coincide with the top-most curve and the corresponding scaling factor was recorded, then the third, and so on, yielding the upper curve in Fig. 1 (b) (designated by open symbols). The same procedure was applied on the metallic side of the transition starting with the highest-density curve, giving the lower curve in Fig. 1 (b) (shown as closed symbols). A quantitative value was assigned to the scaling factor to obtain  $T_0$  for the insulating curves by using the fact that the resistivity of the most insulating (lowest  $n_s$ ) curve was shown (Mason et al, 1995) to exhibit the temperature dependence characteristic of hopping in the presence of a Coulomb gap:  $\rho = \rho_0 \exp(-T_0/T)^{1=2}$  (Efros and Shklovskii 1975).  $T_0$  was determined on the metallic side using the symmetry between metallic and insulating curves, as described in more detail in Kravchenko et al (1995). For all samples studied, this scaling procedure yields a power law dependence of  $T_0$  on  $|n_s - n_c|$  on both sides of the transition:  $T_0 \propto |n_s - n_c|^\alpha$  with the average power  $\alpha = 1.60 \pm 0.1$  for the insulating side and  $1.62 \pm 0.1$  for the metallic side of the transition; this common power law can be clearly seen in the inset to Fig. 1 (b), where for each sample the open (insulating side) and closed (metallic side) symbols form a single line. The same power law was later observed by Popovic (1997) in silicon samples from another source, thus establishing its universality and supporting the validity of the scaling analysis.

Simonian et al (1997a) noted that the metallic and insulating curves are reflection-symmetric in the temperature range between approximately 300 mK and 2 K. In

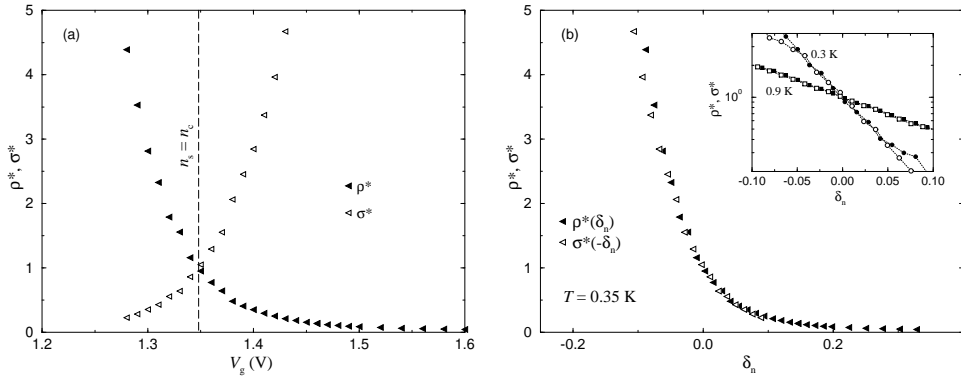


Figure 2. (a) For a silicon MOSFET, the normalized resistivity,  $\rho^*$ , and normalized conductivity,  $\sigma^*$ , as a function of the gate voltage,  $V_g$ , at  $T = 0.35$  K. Note the symmetry about the line  $n_s = n_c$ . The electron density is given by  $n_s = (V_g - 0.58V) \cdot 1.1 \cdot 10^{10} \text{ cm}^{-2}$ . (b) To demonstrate this symmetry explicitly,  $\rho^*(\delta_n)$  (closed symbols) and  $\rho^*(-\delta_n)$  (open symbols) are plotted as a function of  $\delta_n$  ( $n_s - n_c = n_c$ ). Inset:  $\rho^*(\delta_n)$  (closed symbols) and  $\rho^*(-\delta_n)$  (open symbols) versus  $\delta_n$  at  $T = 0.3$  K and  $T = 0.9$  K, the lowest and highest measured temperatures. From Simonian et al (1997a).

Fig. 2 (a), the normalized resistivity,  $\rho^* = \rho/n$ , is shown as a function of the gate voltage,  $V_g$ , together with the normalized conductivity,  $\sigma^* = \sigma/n$ ; the apparent symmetry about the vertical line corresponding to the critical electron density can be clearly seen. Fig. 2 (b) demonstrates that the curves can be mapped onto each other by reflection, i.e.,  $\rho^*(\delta_n)$  is virtually identical to  $\rho^*(-\delta_n)$ . This mapping holds over a range of temperature 0.3 K to 0.9 K; however, the range  $\delta_n$  over which it holds decreases as the temperature is decreased: for example, at  $T = 0.9$  K,  $\rho^*$  and  $\sigma^*$  are symmetric for  $|\delta_n| < 0.1$ , while at  $T = 0.3$  K, they are symmetric only for  $|\delta_n| < 0.05$  (see inset to Fig. 2 (b)). Similar symmetry was later reported by Popovic et al (1997) and Simmons et al (1998). This implies that there is a simple relation between the mechanism for conduction on opposite sides in the vicinity of the transition; the data bear a strong resemblance to the behaviour found by Shahar et al (1996) for the resistivity near the transition between the quantum Hall liquid and insulator, where it has been attributed to charge-flux duality in the composite boson description. It was argued by Dobrosavljevic et al (1997) that both the scaling and reflection symmetry are consequences of a simple analysis assuming that a  $T = 0$  quantum critical point describes the metal-insulator transition.

## 2.2. How universal is $\rho(T)$ ?

The temperature dependence of  $\rho(T)$  is very similar for clean silicon MOSFETs. As an example, Fig. 3 shows the resistivity as a function of temperature of three low-disordered samples obtained from different sources. The behaviour is quantitatively similar in the critical region in the vicinity of the "separatrix", which is the horizontal curve for which the resistivity is independent of temperature. In all samples, the

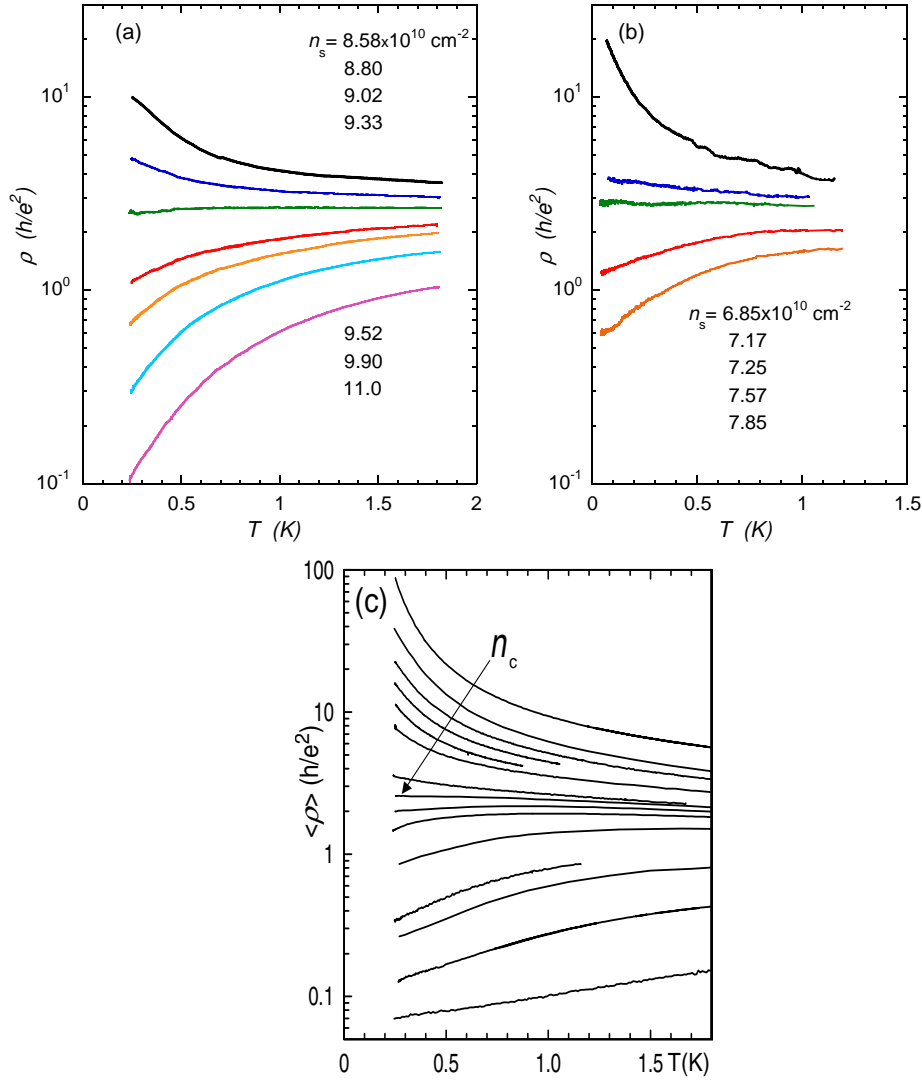


Figure 3. Universal behaviour in ultra-clean silicon MOSFETs: the resistivity versus temperature in three samples from different sources. Note that the resistivities are essentially the same at the separatrices for all samples even though their critical densities are different. (a) high-mobility sample provided by V M Pudalov (graph adopted from Sarachik and Kravchenko 1999), (b) sample fabricated by Heemskerk and Klapwijk (1998) (adopted from Kravchenko and Klapwijk 2000a) and (c) sample of Heemskerk and Klapwijk but from a different wafer (graph adopted from Jaroszynski et al 2002). Electron densities in (c) vary from  $8.55$  to  $14 \cdot 10^{10} \text{ cm}^{-2}$  (top to bottom).

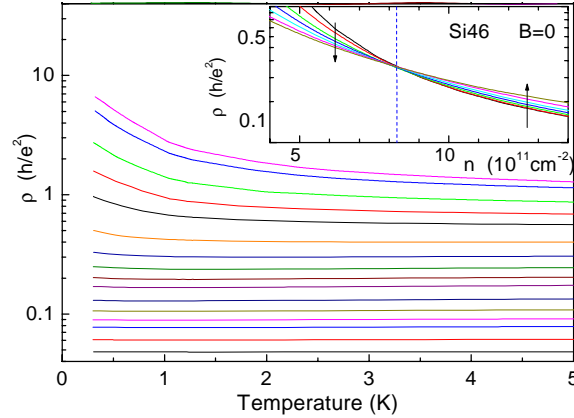


Figure 4. Resistivity versus temperature of a very disordered silicon MOSFET. Note that the vertical scale is similar to Fig. 3. The electron densities are (in units of  $10^{11} \text{ cm}^{-2}$ ): 3.85, 4.13, 4.83, 5.53, 6.23, 7.63, 9.03, 10.4, 11.8, 13.2, 16.0, 18.8, 21.6, 24.4, 30.0 and 37. Adapted from Pudačov et al (2001). Even though there is an apparent crossing point on the  $(n_s)$  isotherms (see the inset), the temperature dependence of the resistivity does not resemble the critical behaviour seen in low-disordered samples.

separatrix is remarkably flat at temperatures below 1 K, and the resistivity is essentially the same numerically at slightly less than  $3h/e^2$ . The curves below the separatrix exhibit strongly metallic temperature dependence ( $d\rho/dT > 0$ ) with no low- $T$  saturation down to the lowest temperature (40 mK or lower; see Fig. 3 (b)); the drop in resistivity reaches as much as a factor of 10 for the bottom curve in Fig. 3 (a). Alternative methods used to determine the critical electron density in low-disordered samples yield the same value as the density for the separatrix (see sec. 2.3). It is important to note that the separatrix in ultra-clean samples represents the "upper limit" of the resistivity for which metallic behaviour (as characterized by  $d\rho/dT > 0$ ) can exist: metallic  $(T)$  has never been observed in any 2D samples at resistivities above  $3h/e^2$ , in quantitative agreement with the predictions of the renormalization group theory (see sec. 5.1).

In more disordered samples, however, the behaviour of the resistivity is very different. Even though the  $(n_s)$  isotherms apparently cross at some electron density (see the inset to Fig. 4), the temperature dependence of the resistivity does not resemble the critical behaviour seen in low-disordered samples. An example of  $(T)$  curves in a disordered sample is shown in Fig. 4. The sample is insulating at electron densities up to  $8 \times 10^{11} \text{ cm}^{-2}$  which is an order of magnitude higher than the critical density in low-disordered samples. The metallic temperature dependence of the resistance visible at higher  $n_s$  does not exceed a few percent (compared to a factor of 10 in low-disordered samples). Most importantly, the density corresponding to the crossing point shown in the inset to Fig. 4 does not coincide with the critical density determined by other methods discussed in the next subsection.

A metal-insulator transition similar to that seen in clean silicon MOSFETs has also been observed in other low-disordered, strongly-interacting 2D systems: p-x At  $T > 2 \text{ K}$ , the resistivity of the separatrix slowly decreases with increasing temperature, as can be seen in Fig. 1, where  $(T)$  curves are shown in a much wider temperature interval.

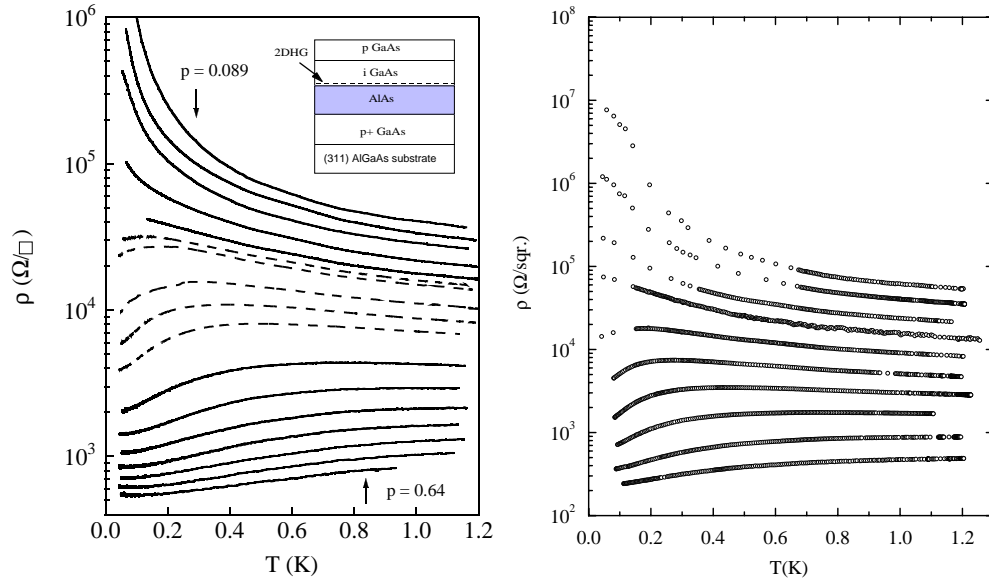


Figure 5. For low-disordered 2D hole systems in p-GaAs/AlGaAs, the resistivity per square is shown as a function of temperature for  $B = 0$  at various fixed hole densities,  $p$ . Left hand panel: ISIS (inverted semiconductor-insulator-semiconductor) structure with hole densities (from top to bottom)  $p = 0.89, 0.94, 0.99, 1.09, 1.19, 1.25, 1.30, 1.50, 1.70, 1.90, 2.50, 3.20, 3.80, 4.50, 5.10, 5.70$  and  $6.40 \times 10^{10} \text{ cm}^{-2}$ . The inset shows a schematic diagram of the ISIS structure: The carriers are accumulated in an undoped GaAs layer situated on top of an undoped AlAs barrier, grown over a  $p^+$  conducting layer which serves as a back-gate; the hole density,  $p$ , is varied by applying a voltage to the back gate. From Hanein et al (1998a). Right hand panel: Temperature dependence of  $\rho$  in an ultra-high mobility p-type GaAs/AlGaAs heterostructure at  $p = 0.48, 0.55, 0.64, 0.72, 0.90, 1.02, 1.27, 1.98, 2.72$  and  $3.72 \times 10^{10} \text{ cm}^{-2}$  (from top to bottom). From Yoon et al (1999).

type SiGe heterostructures (Coleridge et al 1997), GaAs/AlGaAs heterostructures (Hanein et al 1998a; Yoon et al 1999; Mills et al 1999; Noh et al 2002 and others) and AlAs heterostructures (Papadakis and Shayegan 1998). It is difficult to make a direct comparison of the resistivity observed in different material systems because the temperature scales are different, since the Coulomb and Fermi energies depend on the effective mass and carrier density. For example, the characteristic temperature below which the metallic decrease in the resistivity occurs in p-type GaAs/AlGaAs samples is about ten times smaller than in silicon MOSFETs. On the other hand, the values of the resistivity are quite similar in the two systems. In Fig. 5, the resistivity is plotted as a function of temperature for two p-type GaAs/AlGaAs samples produced using different technologies. The data shown in the left hand panel were obtained by Hanein et al (1998a) for an inverted semiconductor-insulator-semiconductor (ISIS) structure with maximum mobility of  $\mu_{\text{max}} = 1.5 \times 10^5 \text{ cm}^2/\text{Vs}$ , while the right-hand panel shows  $\rho(T)$  measured by Yoon et al (1999) on a p-type GaAs/AlGaAs heterostructure with peak mobility by a factor of five higher ( $7 \times 10^5 \text{ cm}^2/\text{Vs}$ ). The interaction parameter,  $r_s$ , changes between approximately 12 and 32 for the left hand

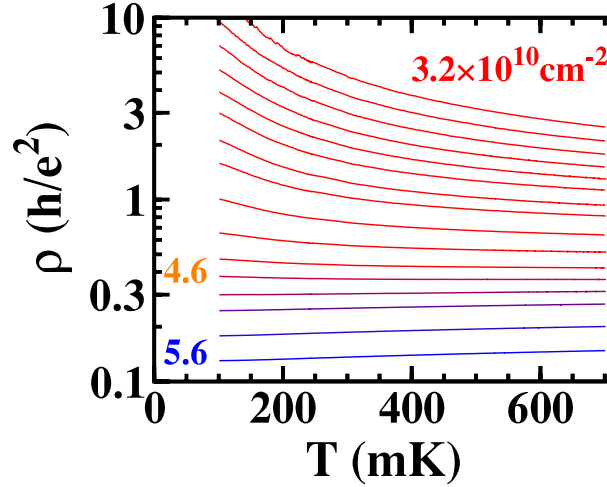


Figure 6. The resistivity as a function of temperature for a disordered p-type GaAs/AlGaAs heterostructure at hole densities  $p = 3.2 \text{--} 5.6 \times 10^{10} \text{ cm}^{-2}$ . From Simmons et al (2000).

plot and from 16 to 44 for the right hand plot. In spite of the difference in the sample quality and range of densities, the dependence of  $\rho(T)$  on temperature is almost the same for the two samples. The main features are very similar to those found in silicon MOSFETs: when the resistivity at "high" temperatures exceeds the quantum resistance,  $h/e^2$  (i.e., at hole densities below some critical value,  $p_c$ ), the  $\rho(T)$  curves are insulating-like in the entire temperature range; for densities just above  $p_c$ , the resistivity shows insulating-like behaviour at higher temperatures and then drops by a factor of 2 to 3 at temperatures below a few hundred mK; and at yet higher hole densities, the resistivity is metallic in the entire temperature range. Note that the curves that separate metallic and insulating behaviour have resistivities that increase with decreasing temperature at the higher temperatures shown; this is quite similar to the behaviour of the separatrix in silicon MOSFETs when viewed over a broad temperature range (see Fig. 1 (a)). However, below approximately 150 mK, the separatrix in p-type GaAs/AlGaAs heterostructures is independent of temperature (Hanein et al., 1998b), as it is in Si MOSFETs below approximately 2 K. The resistivity of the separatrix in both systems extrapolates to  $2/3 h/e^2$  as  $T \rightarrow 0$ , even though the corresponding carrier densities are very different.

As in the case of highly disordered silicon MOSFETs, no critical behaviour of resistance is observed in disordered GaAs/AlGaAs heterostructures. An example is shown in Fig. 6 where the temperature dependence of the resistivity at  $B = 0$  is plotted for hole densities  $p = 3.2 \text{--} 5.6 \times 10^{10} \text{ cm}^{-2}$ . Monotonic localized behaviour is observed even when the "high-temperature" resistivity lies well below  $h/e^2$ , at carrier densities up to  $4.6 \times 10^{10} \text{ cm}^{-2}$ ; both samples shown in the previous figure would be in the deeply metallic regime at this hole density. Above this density, the decrease in resistivity with decreasing temperature is very small (about 10% in the temperature interval 0.7 to 0.1 K).

<sup>k</sup> These  $r_s$  values were calculated assuming that the effective mass is independent of density and equal to  $0.37 m_e$ , where  $m_e$  is the free-electron mass.

As indicated by the experimental results presented above, the  $\rho(T)$  curves are nearly universal in the vicinity of the metal-insulator transition, but only in samples with very weak disorder potential. The strength of the disorder is usually characterized by the maximum carrier mobility,  $\mu_{max}$ . In general, the higher the maximum mobility (i.e. the lower the disorder), the lower the carrier density at which the localization transition occurs. This was shown empirically by Sarachik (2002) to hold over a broad range (five decades in density) for all materials studied: the critical density follows a power law dependence on peak mobility (or scattering rate). However, the data exhibit some scatter, and the correlation is not exact. Thus, for example, the peak hole mobilities in samples used by Hanein et al (1998a) and Simmons et al (1998) are similar, while the localization transition occurs in the latter at a value of  $p$  several times higher than the former. This may be due to sample imperfections (e.g., a slightly inhomogeneous density distribution), which are important at low carrier densities, while the maximum mobility is reached at relatively high carrier densities and may therefore be relatively insensitive to such effects.

A better indicator of the strength of the disorder potential near the MIT is how low the carrier density is at which the localization transition occurs. In silicon MOSFETs, the experimental results obtained to date suggest that the resistivity near the transition approaches universal behaviour for samples in which the transition to a strongly localized state occurs at  $n_s < 10^{10} \text{ cm}^{-2}$ . (In p-type GaAs/AlGaAs heterostructures, the corresponding density separating universal and non-universal behaviour appears to be about an order of magnitude lower, although the data are currently insufficient to determine the value reliably.) Below, we will argue that the "universal" metal-insulator transition in very clean samples is not driven by disorder but by some other mechanism, possibly of magnetic origin. In contrast, the transition is not universal in more disordered samples and is presumably due to Anderson localization, which is strong enough to overpower the metallic behaviour at low densities.

### 2.3. Critical density

To verify whether or not the separatrix corresponds to the critical density, an independent determination of the critical point is necessary: comparison of values obtained using different criteria provides an experimental test of whether or not a true MIT exists at  $B = 0$ . One obvious criterion, hereafter referred to as the "derivative criterion", is a change in sign of the temperature derivative of the resistivity,  $d\rho/dT$ ; this is the criterion often used to identify the MIT. A positive (negative) sign of the derivative at the lowest achievable temperatures is empirically associated with a metallic (insulating) phase. A weakness of this criterion is that it requires extrapolation to zero temperature. A second criterion can be applied based on an analysis of a temperature-independent characteristic, namely, the localisation length  $L$  extrapolated from the insulating phase. These two methods have been applied to low-disordered silicon MOSFETs by Shashkin et al (2001b) and Jaroszynski et al (2002).

As mentioned earlier, the temperature dependence of the resistance deep in the insulating phase obeys the Efros-Shklovskii variable-range hopping form (Mason et al 1995); on the other hand, closer to the critical electron density at temperatures that are not too low, the resistance has an activated form  $\rho \sim \exp(E_a/k_B T)$  (Pepper et al 1974; Pudalov et al 1993; Shashkin et al 1994) due to thermal activation to the mobility

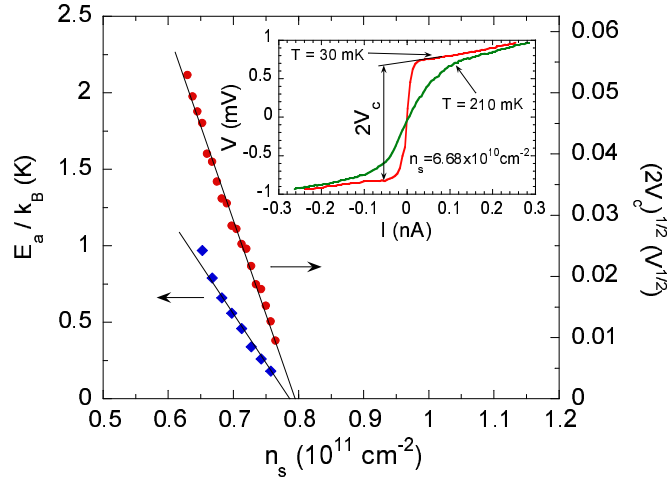


Figure 7. Activation energy (diamonds) and square root of the threshold voltage (circles) versus electron density in zero magnetic field in a low-disordered silicon MOSFET. The inset shows current-voltage characteristics recorded at 30 and 210 mK, as labeled; note that the threshold voltage is essentially independent of temperature. From Shashkin et al (2001b).

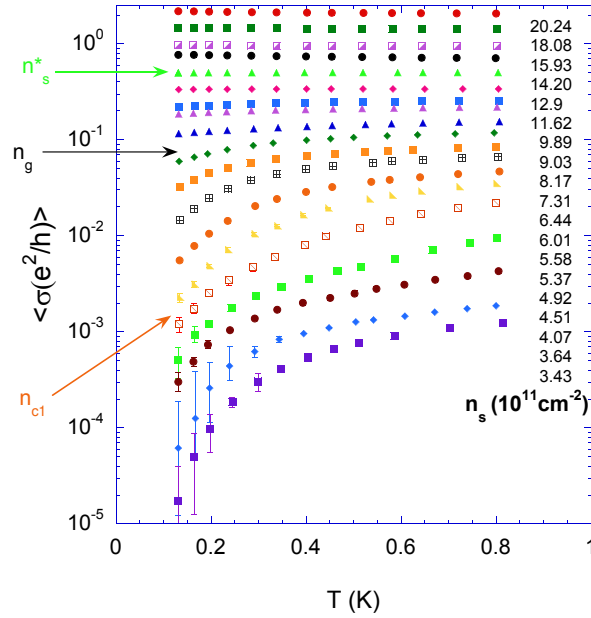


Figure 8. Conductivity versus temperature for different  $n_s$  in a highly disordered silicon MOSFET. (The error bars show the size of the fluctuations of the conductivity with time.) The critical electron densities obtained by the derivative and localization length criteria ( $n_s^*$  and  $n_{cl}$ , correspondingly) are marked by arrows.  $n_g$  is the density corresponding to the onset of glassy behaviour; see text. The figure is adopted from Bogdanovich and Popovic (2002).

edge. Fig. 7 shows the activation energy  $E_a$  as a function of the electron density (diamonds); the data can be approximated by a linear function which yields, within the experimental uncertainty, the same critical electron density as the "derivative criterion".

The critical density can also be determined by studying the nonlinear current-voltage  $I-V$  characteristics on the insulating side of the transition. A typical low-temperature  $I-V$  curve is close to a step-like function: the voltage rises abruptly at low current and then saturates, as shown in the inset to Fig. 7; the magnitude of the step is  $2V_c$ . The curve becomes less sharp at higher temperatures, yet the threshold voltage,  $V_c$ , remains essentially unchanged. Closer to the MIT, the threshold voltage decreases, and at  $n_s = n_{c1} = 0.795 \times 10^{10} \text{ cm}^{-2}$ , the  $I-V$  curve is strictly linear (Shashkin et al 2001b). According to Polyakov and Shklovskii (1993) and Shashkin et al (1994), the breakdown of the localized phase occurs when the localized electrons at the Fermi level gain enough energy to reach the mobility edge in an electric field,  $V_c = d$ , over a distance given by the localization length,  $L$ , which is temperature-independent:

$$eV_c(n_s) L(n_s) = d = E_a(n_s)$$

(here  $d$  is the distance between the potential probes). The dependence of  $V_c^{1=2}(n_s)$  near the MIT is linear, as shown in Fig. 7 by closed circles, and its extrapolation to zero threshold value again yields approximately the same critical electron density as the two previous criteria. The linear dependence  $V_c^{1=2}(n_s)$ , accompanied by linear  $E_a(n_s)$ , signals the localization length diverging near the critical density:  $L(n_s) \propto 1/(n_c - n_s)$ .

These experiments indicate that in low-disordered samples, the two methods—one based on extrapolation of  $(T)$  to zero temperature and a second based on the behaviour of the temperature-independent localization length—give the same critical electron density:  $n_c = n_{c1}$ . This implies that the separatrix remains "flat" (or extrapolates to a finite resistivity) at zero temperature. Since one of the methods is independent of temperature, this equivalence supports the existence of a true  $T = 0$  MIT in low-disordered samples in zero magnetic field.

In contrast, we note that in highly-disordered samples, the localization length method yields a critical density noticeably lower than the derivative criterion. Figure 8 shows the (time-averaged) conductivity  $\sigma$  as a function of  $T$  for different  $n_s$ .  $d\sigma/dT$  changes sign at electron density  $n_s = 12.9 \times 10^{10} \text{ cm}^{-2}$ . The activation energy, however, vanishes at  $n_{c1} = 5.2 \times 10^{10} \text{ cm}^{-2}$ , which is more than a factor of two lower than  $n_s$ : at densities between these two values, the resistivity does not diverge as  $T \rightarrow 0$ , even though it exhibits an insulating-like temperature dependence. Thus, these two different methods yield different "critical densities" for a sample with strong disorder. Moreover, from the study of low-frequency resistance noise in dilute silicon MOSFETs, Bogdanovich and Popovic (2002) and Jaroszynski et al (2002) have found that the behaviour of several spectral characteristics indicates a dramatic slowing down of the electron dynamics at a well-defined electron density  $n_g$ , which they have interpreted as an indication of a (glassy) freezing of the 2D electron system. In low-disordered samples,  $n_g$  nearly coincides with  $n_c$ , while in highly-disordered sample,  $n_g$  lies somewhere between  $n_{c1}$  and  $n_s$ , as indicated in Fig. 8. The width of the glass phase ( $n_{c1} < n_s < n_g$ ) thus strongly depends on disorder, becoming extremely narrow (or perhaps even vanishing) in low-disordered samples. The strong dependence on disorder of the width of the metallic glass phase is consistent with predictions of the model of interacting electrons near a disorder-driven metal-insulator transition

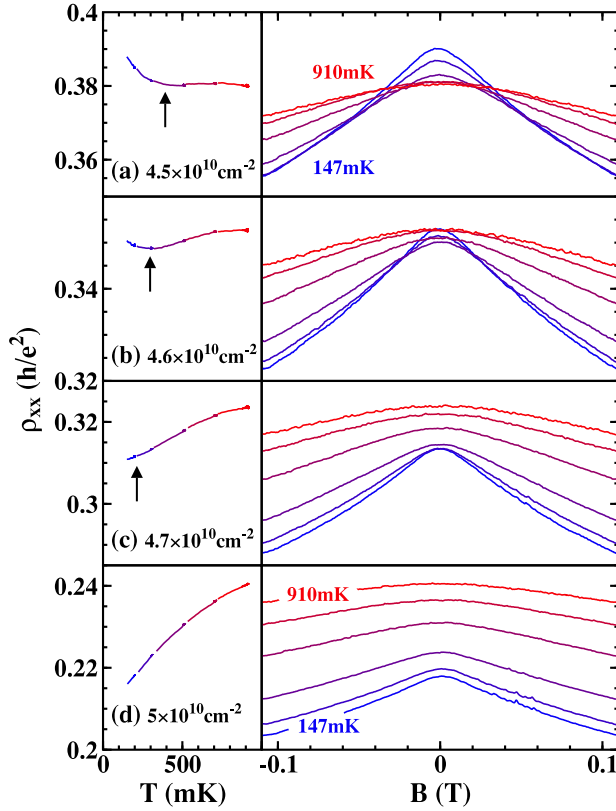


Figure 9. (a-d) The left hand panels show data for the resistivity versus temperature at  $B = 0$  in a disordered p-type GaAs/AlGaAs quantum well, illustrating the transition from insulating to metallic behaviour as the density increases. The right hand panels show the corresponding magnetoresistance traces for temperatures of 147, 200, 303, 510, 705, and 910 mK. From Simmons et al (2000).

(Pastor and Dobrosavljevic 1999). These observations all suggest that the origin of the metal-insulator transition is different in clean and strongly-disordered samples.

#### 2.4. Does weak localization survive in the presence of strong interactions?

The theory of weak localization was developed for noninteracting systems, and it was not a priori clear whether it would work in the presence of strong interactions. In 2000, Simmons et al studied transport properties of a dilute modulation-doped p-type GaAs/AlGaAs quantum well and observed a temperature-dependent negative magnetoresistance, consistent with the suppression of the coherent backscattering by the perpendicular magnetic field. Magnetoresistance curves obtained by Simmons et al are plotted in the right hand panel of Fig. 9. A characteristic peak develops in the resistivity at  $B = 0$  as the temperature is decreased, signalling that the weak localization is still present at  $p$  as low as  $4.5 \times 10^{10} \text{ cm}^{-2}$ , corresponding to the interaction parameter  $r_s = 15$ . Simmons et al successfully fitted their

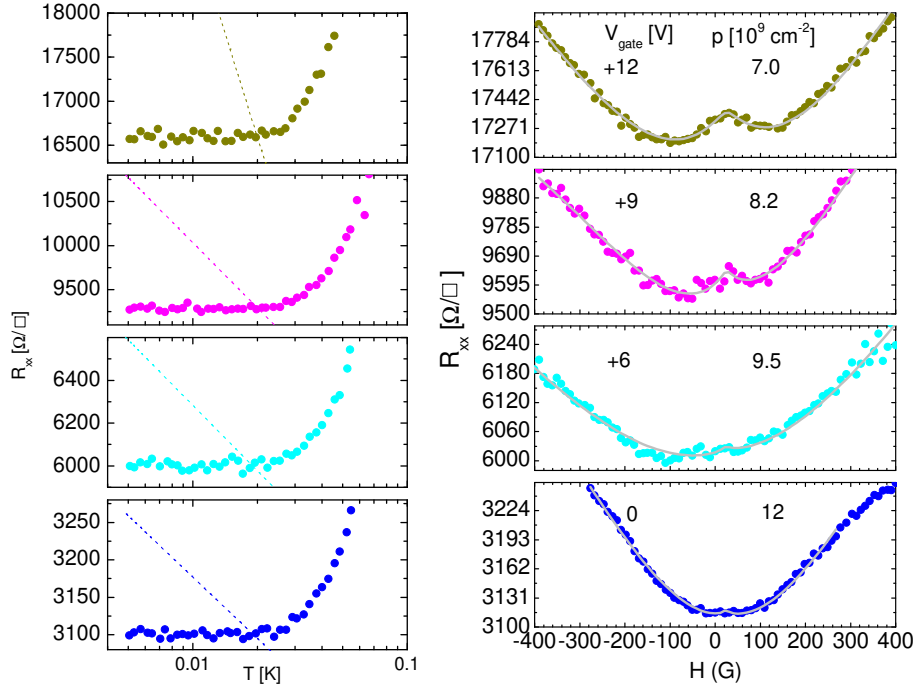


Figure 10. The left hand panels show resistance per square as a function of temperature for 2D holes in an ultra-clean GaAs/AlGaAs heterostructure for various values of the gate bias. The right hand panels show the variation of longitudinal resistance with perpendicular magnetic field for the same sample at various gate biases. The solid grey lines represent the fit described in the text. From Mills et al (2001).

magnetoconductance data by the Hikami-Larkin formula (Hikami et al 1980)

$$\sigma = \frac{e^2}{h} \left( \frac{1}{2} + \frac{B}{B_0} \right) \left( \frac{1}{2} + \frac{B}{B_0} \right); \quad (1)$$

and obtained reasonable values of the phase-breaking time,  $\tau_{ph}$  10 to 30 ps, in the temperature interval 1 to 0.15 K (here  $\tau_{ph}$  is the elastic scattering time,  $\gamma$  is the Dirac gamma function,  $B_0 = h/4eB_0 D$ , and  $D$  is the diffusion coefficient). Weak negative magnetoconductance was also observed by Brunthaler et al (2001) in silicon MOSFETs at electron densities down to  $1.5 \times 10^{10} \text{ cm}^{-2}$ , although they found values of  $\tau_{ph}$  that were about an order of magnitude shorter than those expected theoretically,  $\tau_{ph}^2 = e^2 k_B T$ .

However, the agreement with non-interacting theory breaks down at higher interaction strengths. Mills et al (2001) studied p-type GaAs/AlGaAs heterostructures of much higher quality which remained metallic down to  $p = 3 \times 10^{10} \text{ cm}^{-2}$  (corresponding to  $r_s = 60$  provided the effective mass does not change), and found the coherent backscattering to be almost completely suppressed at these ultra-low hole densities. In the right hand panel of Fig. 10, the magnetoconductance traces are shown at  $T = 9 \text{ mK}$  for four different carrier densities. The width of the characteristic peak at  $B_0 = 0$ , visible in the top two curves, is approximately as expected from the theory,

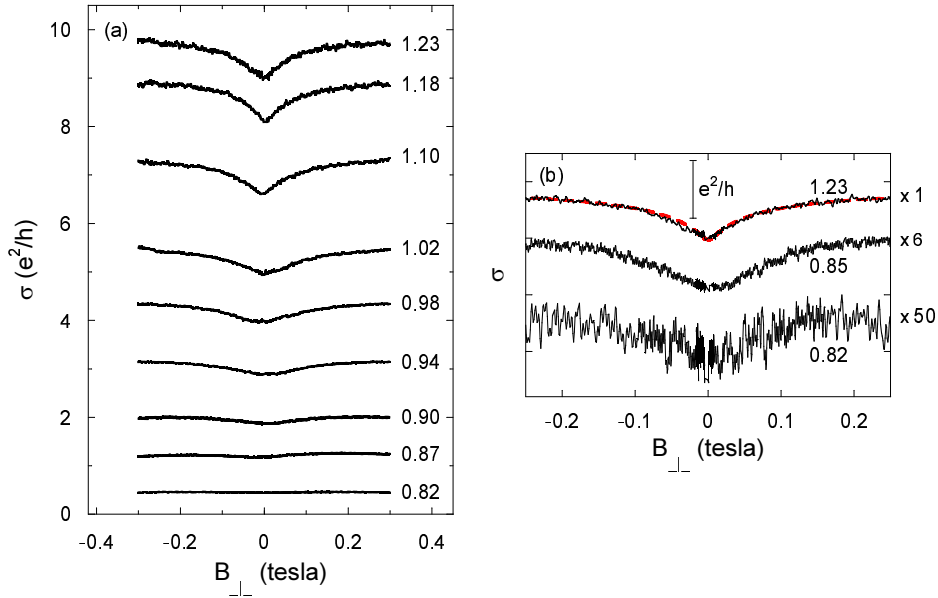


Figure 11. Longitudinal magnetoconductivity of a low-disordered silicon MOSFET in a weak perpendicular magnetic field at  $T = 42$  mK for a range of electron densities indicated near each curve in units of  $10^{11}$   $\text{cm}^{-2}$ . The curves in (b) are vertically shifted and the two lowest curves are multiplied by 6 (the middle one) and 50 (the lower one). The thick dashed line in (b) is a fit by Eq. 1 with  $b = 0.6$  and  $\tau = 30$  ps. From Rahimiet al (2003).

but its magnitude is about a factor of 30 smaller than expected. At slightly higher  $n_s$  (the two bottom curves), the peak is not seen at all.

In principle, the strong disagreement between the expected and measured peak magnitudes might be due to the fact that the theory for coherent backscattering is not applicable to a system with resistivity of the order of  $h/e^2$ . However, this is not the source of the disagreement, as the resistivity in the experiments of Mills et al (2001) is in the same range as in the experiments of Simmons et al (2000) (cf Figs. 9 and 10). Therefore the suppression of the peak is apparently related to stronger interactions (higher  $r_s$ ) in the Mills et al samples rather than to high values of  $b$ .

The left hand panel of Fig. 10 shows the temperature dependence of the  $B = 0$  resistance in the ultra low density sample of Mills et al over the temperature range 5 to 100 mK. The dashed lines show the expected corrections to the resistivity caused by weak localization calculated using the equation  $\rho(T) = b e^2/h \ln(\tau/T)$ , where  $b$  is a constant expected to be universal and equal to  $1/2$ . The calculated dependence is clearly at variance with the measurements; rather, at very low temperatures, the resistance becomes nearly constant. Fitting the theoretical expression to the experimental data, Mills et al found that the upper limits for  $b$  are from one to nearly two orders of magnitude smaller than the  $b = 1/2$  expected from the theory.

The disappearance of weak localization corrections near the MIT has also been observed by Rahimiet al (2003) in low-disordered silicon MOSFETs. The results are shown in Fig. 11. At higher  $n_s$  (the upper curves in Fig. 11 (a)), the characteristic dip is observed in the magnetoconductance at zero magnetic field. As follows from Eq. 1,

the magnitude of the dip is expected to be equal to  $(be^2g_v/h) \ln(\epsilon)$ , and should therefore exhibit a weak (double-logarithmic) increase as the average conductivity decreases provided the variations in electron density are small, as they are in this case. This is not what is observed in the experiment: as one approaches the transition, the magnitude of the dip decreases sharply, and at the critical electron density (the lowest curve in Fig. 11 (a)), the dip is no longer seen on the scale of this figure. However, the shape of the magnetoconductivity does not change significantly with decreasing  $n_s$  as illustrated by the middle curve in Fig. 11 (b), which shows  $(B_{\parallel})$  multiplied by six ( $n_s = 0.85 \times 10^{10} \text{ cm}^{-2}$ ) to make it quantitatively similar to the upper curve. This similarity demonstrates that the functional form of the  $(B_{\parallel})$  dependence, described by the expression in square brackets in Eq. 1, does not change noticeably as the density is reduced from  $1.23 \times 10^{10}$  to  $0.85 \times 10^{10} \text{ cm}^{-2}$ ; instead, it is the magnitude of the effect that rapidly decreases upon approaching the MIT. At yet lower density,  $n_s = 0.82 \times 10^{10} \text{ cm}^{-2}$ , the magnitude of the dip does not exceed 2% of that for  $n_s = 1.23 \times 10^{10} \text{ cm}^{-2}$  (compare the upper and the lower curves in Fig. 11 (b)).

It may seem surprising that a change in  $n_s$  by only a factor of 1.5 (from  $n_s = 1.23 \times 10^{10}$  to  $n_s = 0.82 \times 10^{10} \text{ cm}^{-2}$ ) results in such a dramatic suppression of the quantum localization. It is interesting to note in this connection that the experimental data on silicon MOSFETs described in sections 4.2 and 4.3 reveal a sharp increase of the effective mass in the same region of electron densities where the suppression of the weak localization is observed. Due to the strong renormalization of the effective mass, the ratio between the Coulomb and Fermi energies,  $r = 2r_s(m^*m_b)$ , grows much faster than  $n_s^{-1/2}$  reaching values greater than 50 near the critical density.

The apparent absence of localization at and just above the critical density may account for the existence of a stable separatrix at  $n_s = n_c$  (see Fig. 3). If the localization were present, the temperature-independent curve would require that the temperature dependence of  $\sigma$  due to localization be cancelled exactly over a wide temperature range by a temperature dependence of opposite sign due to interactions, a coincidence which seems very improbable for two unrelated mechanisms. Note that at resistivity levels of order or greater than  $h/e^2$ , the quantum corrections to the resistivity are expected to be very strong and cannot be easily overlooked. The calculated temperature dependence of the resistivity, expected for non-interacting electrons (Abraham et al 1979), is shown in Fig. 12 by the dashed curve: at 100 mK, quantum localization is expected to cause a factor of more than 30 increase in resistivity, in strong contradiction with the experiment which shows it to be constant within 5%.

### 3. THE EFFECT OF A MAGNETIC FIELD

#### 3.1. Resistance in a parallel magnetic field

In ordinary metals, the application of a parallel magnetic field ( $B_{\parallel}$ ) does not lead to any dramatic changes in the transport properties: if the thickness of the 2D electron system is small compared to the magnetic length, the parallel field couples largely to the electrons' spins while the orbital effects are suppressed. Only weak corrections to the conductivity are expected due to electron-electron interactions (Lee and Ramakrishnan 1982, 1985). It therefore came as a surprise when Dolgoplov et al (1992) observed a dramatic suppression of the conductivity in dilute Si MOSFETs by a parallel in-plane magnetic field  $B_{\parallel}$ . The magnetoresistance in a parallel field was studied in detail by Simonian et al (1997b) and Pudalov et al (1997), also in Si

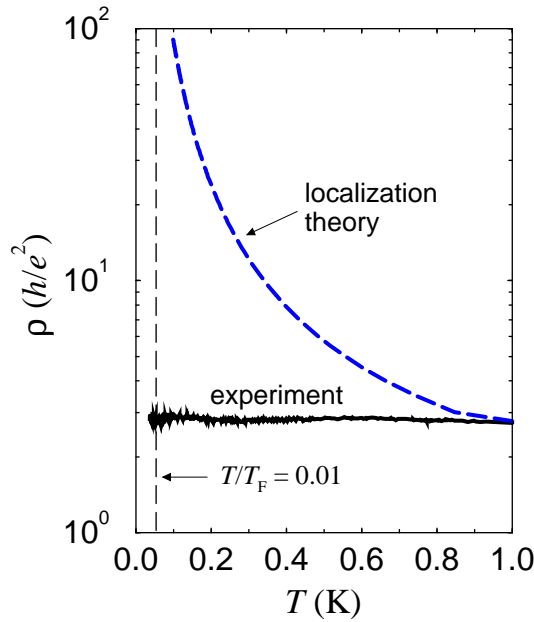


Figure 12. Resistivity at the separatrix in a low-disordered silicon MOSFET as a function of temperature (the solid curve) compared to that calculated from the one-parameter scaling theory using  $\frac{d \ln \rho(L)}{d \ln L} = \frac{1}{2} - \frac{1}{2} \ln(1 + a)$  (here  $L / T^{p=2}$  is the phase-breaking length,  $\ln(1 + a)$  is the scaling function approximated by  $\ln(1 + a)$  following Altshuler et al (2000),  $a = 2 = \frac{1}{\nu}$ ,  $\nu$  is measured in units of  $h/e^2$ , and  $p$  and  $\nu$  are constants equal to 3 and 0.5 respectively). As the dashed line shows, the resistivity of a "conventional" (noninteracting) 2D system should have increased by a factor of more than 30 when the temperature has been reduced to 100 mK. From Kravchenko and Lapwijk (2000a).

MOSFETs. In the left hand part of Fig. 13, the resistivity is shown as a function of parallel magnetic field at a fixed temperature of 0.3 K for several electron densities. The resistivity increases sharply as the magnetic field is raised, changing by a factor of about 4 at the highest density shown and by more than an order of magnitude at the lowest density, and then saturates and remains approximately constant up to the highest measuring field,  $B_k = 12$  tesla. The magnetic field where the saturation occurs,  $B_{sat}$ , depends on  $n_s$ , varying from about 2 tesla at the lowest measured density to about 9 tesla at the highest. The metallic conductivity is suppressed in a similar way by magnetic fields applied at any angle relative to the 2D plane (Kravchenko et al 1998) independently of the relative directions of the measuring current and magnetic field (Simonian et al 1997b; Pudalov et al 2002a). All these observations suggest that the giant magnetoresistance is due to coupling of the magnetic field to the electrons' spins. Indeed, from an analysis of the positions of Shubnikov-de Haas oscillations in tilted magnetic fields, Okamoto et al (1999) and Vitkalov et al (2000, 2001a) have concluded that in MOSFETs at relatively high densities, the magnetic field  $B_{sat}$  is equal to that required to fully polarize the electrons' spins.

In p-type GaAs/AlGaAs heterostructures, the effect of a parallel magnetic field is qualitatively similar, as shown in the right hand part of Fig. 13. The dependence

Metal-insulator transition in 2D

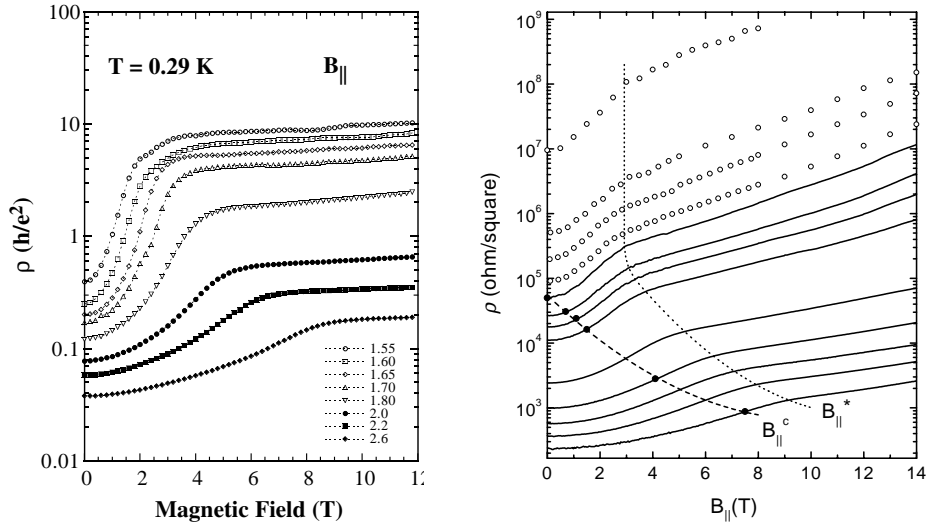


Figure 13. Left hand panel: resistivity versus parallel magnetic field measured at  $T = 0.29$  K on low-disordered silicon sample. Different symbols correspond to densities from  $1.01$  to  $2.17 \times 10^{11} \text{ cm}^{-2}$  (adopted from Pudalov et al 1997). Right hand panel: resistivity as a function of  $B_{||}$  in a p-GaAs/AlGaAs heterostructure at  $50$  mK at the following hole densities, from the bottom:  $4.11, 3.23, 2.67, 2.12, 1.63, 1.10, 0.98, 0.89, 0.83, 0.79, 0.75, 0.67 \times 10^{10} \text{ cm}^{-2}$ . The solid lines are for hole densities above  $p_c$  and the open circles are for densities below  $p_c$ . The solid circles denote the experimentally determined critical magnetic fields, and the dashed line is a guide to the eye.  $B_{||}^c$ , the boundary separating the high and the low field regions, is shown by the dotted line. Adopted from Yoon et al (2000).

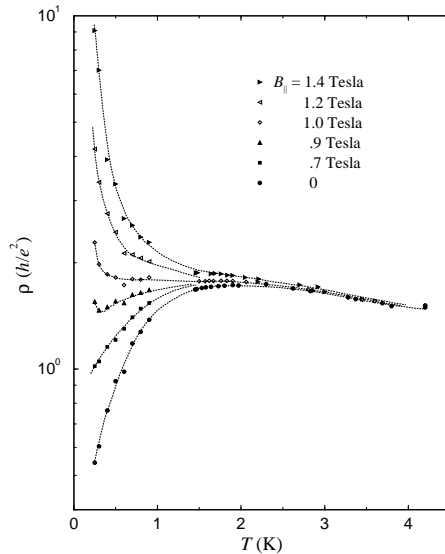


Figure 14. Resistivity versus temperature for various parallel magnetic fields applied parallel to the plane of a low-disordered silicon MOSFET. The electron density is  $8.83 \times 10^{10} \text{ cm}^{-2}$ . From Simonian et al (1997b).

of  $\rho_{xx}$  does not saturate to a constant value as in Si MOSFETs, but continues to increase with increasing  $\mu_0 H_{\parallel}$ , albeit at a considerably slower rate. This is presumably due to strong coupling of the parallel  $\mu_0 H_{\parallel}$  to the orbital motion arising from the finite layer thickness (see Das Sarma and Hwang 2000), an effect that is more important in GaAs/AlGaAs heterostructures than in silicon MOSFETs because of a much thicker layer. As in the case of Si MOSFETs, there is a distinct knee that serves as a demarcation between the behaviour in low and high  $\mu_0 H_{\parallel}$ . For high hole densities, Shubnikov-de Haas measurements (Tutuc et al 2001) have shown that this knee is associated with full polarization of the spins by the in-plane magnetic  $\mu_0 H_{\parallel}$ . However, unlike Si MOSFETs, the magnetoresistance in p-GaAs/AlGaAs heterostructures has been found to depend on the relative directions of the measuring current, magnetic  $\mu_0 H_{\parallel}$ , and crystal orientation (Papadakis et al 2000); one should note that the crystal anisotropy of this material introduces added complications. In p-SiGe heterostructures, the parallel  $\mu_0 H_{\parallel}$  was found to induce negligible magnetoresistance (Senz et al 1999) because in this system the parallel  $\mu_0 H_{\parallel}$  cannot couple to the spins due to very strong spin-orbit interactions.

Over and above the very large magnetoresistance induced by an in-plane magnetic  $\mu_0 H_{\parallel}$ , an even more important effect of a parallel  $\mu_0 H_{\parallel}$  is that it causes the zero- $\mu_0 H_{\parallel}$  2D metal to become an insulator (Simonian et al 1997b; Mertes et al 2001; Shashkin et al 2001b; Gao et al 2002). Figure 14 shows how the temperature dependence of the resistance changes as the magnetic  $\mu_0 H_{\parallel}$  is increased. Here, the resistivity of a Si MOSFET with fixed density on the metallic side of the transition is plotted as a function of temperature in several fixed parallel magnetic  $\mu_0 H_{\parallel}$  between 0 and 1.4 tesla. The zero- $\mu_0 H_{\parallel}$  curve exhibits behaviour typical for "just-metallic" electron densities: the resistivity is weakly-insulating at  $T > T_{max} \approx 2$  K and drops substantially as the temperature is decreased below  $T_{max}$ . In a parallel magnetic  $\mu_0 H_{\parallel}$  of only 1.4 tesla (the upper curve), the metallic drop of the resistivity is completely suppressed, so that the system is now strongly insulating in the entire temperature range. The effect of the  $\mu_0 H_{\parallel}$  is negligible at temperatures above  $T_{max}$ , i.e., above the temperature below which the metallic behaviour in  $B = 0$  sets in.

The extreme sensitivity to parallel  $\mu_0 H_{\parallel}$  is also illustrated in Fig. 15 where the temperature dependence of the resistivity is compared in the absence (a) and in the presence (b) of a parallel magnetic  $\mu_0 H_{\parallel}$ . For  $B_k = 0$ , the resistivity displays the familiar, nearly symmetric (at temperatures above 0.2 K) critical behaviour about the separatrix (the dashed line). However, in a parallel magnetic  $\mu_0 H_{\parallel}$  of  $B_k = 4$  tesla, which is high enough to cause full spin polarization at this electron density, all the  $\rho_{xx}(T)$  curves display "insulating-like" behaviour, including those which start below  $\nu = e^2/h$  at high temperatures. There is no temperature-independent separatrix at any electron density in a spin-polarized electron system (Simonian et al 1997b; Shashkin et al 2001b).

This qualitative difference in behaviour demonstrates convincingly that the spin-polarized and unpolarized states behave very differently. This rules out explanations which predict qualitatively similar behaviour of the resistance regardless of the degree of spin polarization. In particular, the explanation of the metallic behaviour suggested by Das Sarma and Hwang (1999) (see also Lilly et al 2003), based on the temperature-dependent screening, predicts metallic-like  $\rho_{xx}(T)$  for both spin-polarized and unpolarized states, which is in disagreement with experiment (for more on this discrepancy, see Mertes et al 2001).

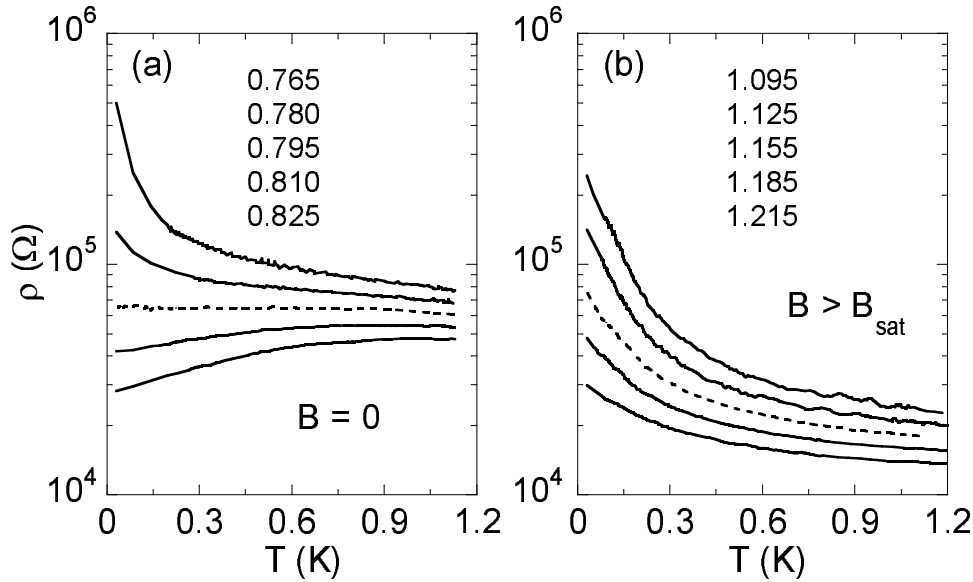


Figure 15. Temperature dependence of the resistivity of a low-disordered silicon MOSFET at different electron densities near the MIT in zero magnetic field (a), and in a parallel magnetic field of 4 tesla (b). The electron densities are indicated in units of  $10^{11} \text{ cm}^{-2}$ . Dashed curves correspond to  $n_s = n_{c1}$  which is equal to  $0.795 \cdot 10^{11} \text{ cm}^{-2}$  in zero field and to  $1.155 \cdot 10^{11} \text{ cm}^{-2}$  in  $B_k = 4$  tesla. From Shashkin et al (2001b).

### 3.2. Scaling of the magnetoresistance; evidence for a phase transition

There have been many attempts to obtain a quantitative description of the magnetoresistance as a function of the carrier density and temperature over the entire field range, including the saturation region. Attempts to obtain a collapse of the magnetoresistance onto a single scaled curve have yielded scaling at either low or high magnetic field; over a wide range of temperatures but only at the metal-insulator transition; or in a wide range of carrier densities, but only in the limit of very low temperatures. Simonian et al (1998) found that at the transition, the deviation of the magnetoresistance from its zero-field value,  $\rho(B_k) - \rho(0)$ , is a universal function of  $B_k/T$ . Although the quality of the scaling is good, it breaks down rather quickly as one moves into the metallic phase.

Two scaling procedures have been recently proposed; although they differ in procedure and yield results that differ somewhat in detail, the major conclusions are essentially the same, as described below, and imply that there is an approach to a quantum phase transition at a density near  $n_c$ .

Shashkin et al (2001a) scaled the magnetoresistivity in the spirit of the theory of Dolgoplov and Gold (2000), who predicted that at  $T = 0$ , the normalized magnetoresistance is a universal function of the degree of spin polarization,  $P = g_B B_k / 2E_F = g m_B B_k / h^2 n_s$  (here  $m$  is the effective mass and  $g$  is the  $g$ -factor). Shashkin et al scaled the data obtained in the limit of very low temperatures where the magnetoresistance becomes temperature-independent and, therefore, can be considered to be at its  $T = 0$  value. In this regime, the normalized magnetoresistance,

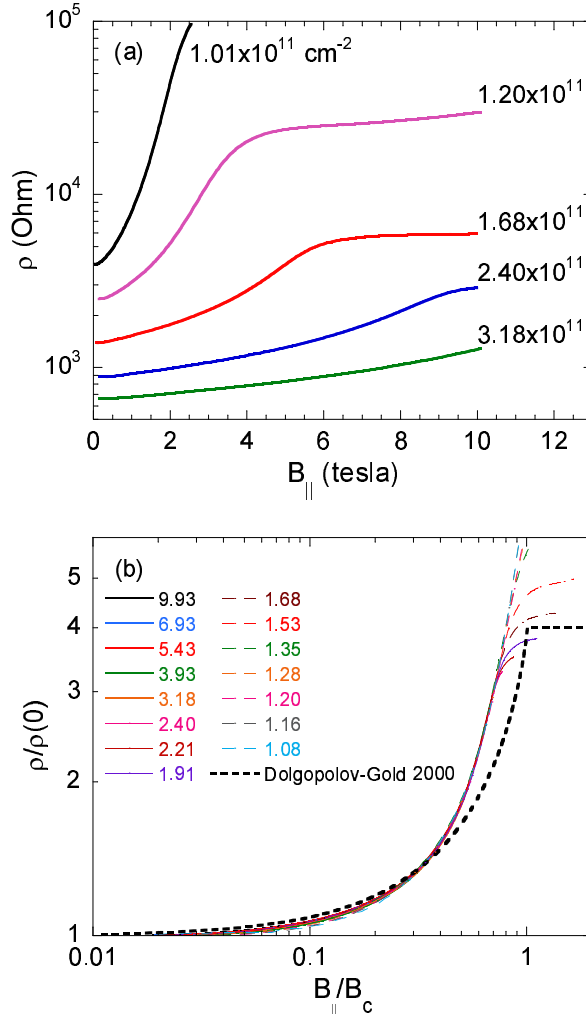


Figure 16. (a) Low-temperature magnetoresistance of a clean silicon MOSFET in parallel magnetic field at different electron densities above  $n_c$ . (b) Scaled curves of the normalized magnetoresistance versus  $B_{||}/B_c$ . The electron densities are indicated in units of  $10^{11} \text{ cm}^{-2}$ . Also shown by a thick dashed line is the normalized magnetoresistance calculated by Dolgoplov and Gold (2000). Adapted from Shashkin et al (2001a).

$\rho(B_{||}) = \rho(0)$ , measured at different electron densities, collapses onto a single curve when plotted as a function of  $B_{||}/B_c$  (here  $B_c$  is the scaling parameter, normalized to correspond to the magnetic field  $B_{sat}$  at which the magnetoresistance saturates). An example of how  $\rho(B_{||})$ , plotted in Fig. 16 (a), can be scaled onto a universal curve is shown in Fig. 16 (b). The resulting function is described reasonably well by the theoretical dependence predicted by Dolgoplov and Gold. The quality of the scaling is remarkably good for  $B_{||}/B_c = 0.7$  in the electron density range  $1.08 \times 10^{11}$  to  $10 \times 10^{11} \text{ cm}^{-2}$ , but it breaks down as one approaches the metal-insulator transition where the magnetoresistance becomes strongly temperature-dependent even at the

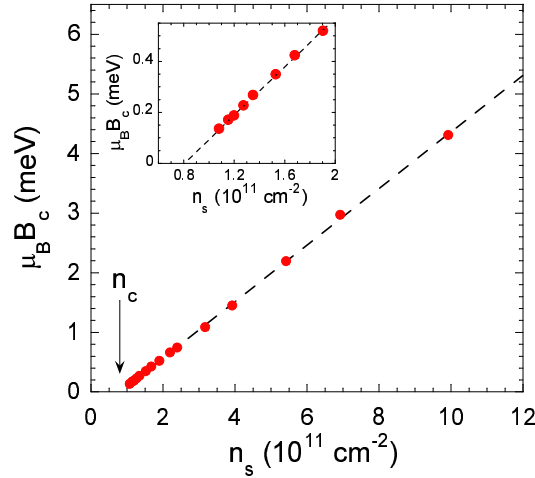


Figure 17. Scaling parameter  $B_c$  (corresponding to the field required for full spin polarization) as a function of the electron density. An expanded view of the region near  $n_c$  is displayed in the inset. From Shashkin et al (2001a).

lowest experimentally achievable temperatures. As shown in Fig. 17, the scaling parameter is proportional over a wide range of electron densities to the deviation of the electron density from its critical value:  $B_c / (n_s - n_c)$ .

Vitkalov et al (2001b) succeeded in obtaining an excellent collapse of magnetoconductivity data over a broad range of electron densities and temperatures using a single scaling parameter. They separated the conductivity into a field-dependent contribution,  $\sigma_k(B_k)$  (1), and a contribution that is independent of magnetic field,  $\sigma_0$  (1). The field-dependent contribution to the conductivity,  $\sigma_k(B_k)$ , normalized to its full value,  $\sigma_k(B_k=B_c)$  (1), was shown to be a universal function of  $B/B_c$ :

$$\frac{\sigma_k(B_k)}{\sigma_k(B_k=B_c)} = F(B_k/B_c) \quad (2)$$

where  $B_c(n_s; T)$  is the scaling parameter. Applied to the magnetoconductance curves shown in Fig. 18 (a) for different electron densities, the above scaling procedure yields the data collapse shown in Fig. 18 (b).

Remarkably, similar scaling holds for curves obtained at different temperatures. This is demonstrated in Fig. 19, which shows the scaled magnetoconductance measured at a fixed density and different temperatures. Altogether, the scaling holds for temperatures up to 1.6 K over a broad range of electron densities up to  $4n_c$ .

Fig. 20 shows the scaling parameter  $B_c$  plotted as a function of temperature for different electron densities  $n_s > n_c$ . The scaling parameter becomes smaller as the electron density is reduced; for a given density,  $B_c$  decreases as the temperature decreases and approaches a value that is independent of temperature,  $B_c(T = 0)$ . As the density is reduced toward  $n_c$ , the temperature dependence of  $B_c$  dominates over a broader range and becomes stronger, and the low-temperature asymptotic value becomes smaller. Note that for electron densities below  $1.36 \times 10^{11} \text{ cm}^{-2}$ ,  $B_c$  is approximately linear with temperature at high T. The behaviour of the scaling

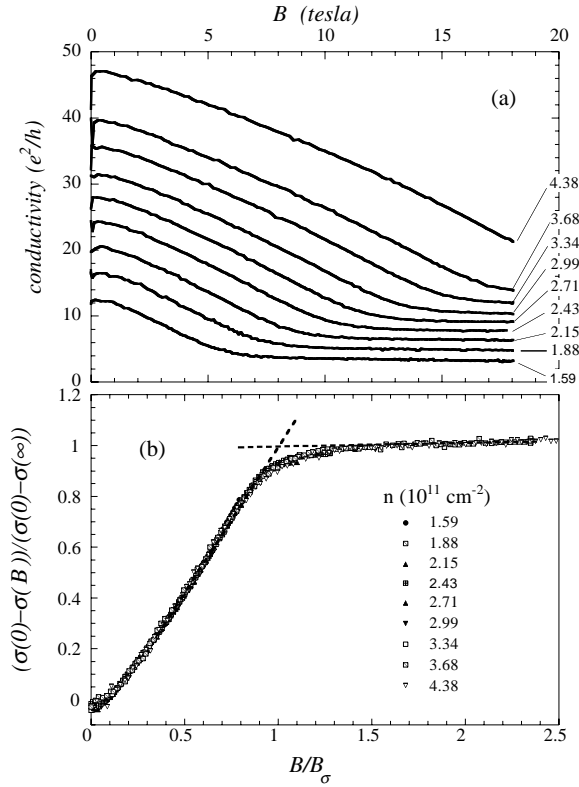


Figure 18. (a) Conductivity of a low-disordered silicon sample versus in-plane magnetic field at different electron densities in units of  $10^{11} \text{ cm}^{-2}$ , as labelled;  $T = 100 \text{ mK}$ . (b) Data collapse obtained by applying the scaling procedure, Eq 2, to the curves shown in (a). Adapted from Vitkalov et al (2001b).

parameter  $B_c(T)$  can be approximated by an empirical fitting function:

$$B_c(n_s; T) = A(n_s) [(n_s)^2 + T^2]^{-1/2}$$

The solid lines in Fig. 20 (a) are fits to this expression using  $A(n_s)$  and  $(n_s)$  as fitting parameters. As can be inferred from the slopes of the curves of Fig. 20 (a), the parameter  $A(n_s)$  is constant over most of the range and then exhibits a small increase (less than 20%) at lower densities. As shown in Fig. 20 (b), the parameter  $A(n_s)$  decreases sharply with decreasing density and extrapolates to zero at a density  $n_0$  which is within 10% of the critical density  $n_c = 0.85 \times 10^{11} \text{ cm}^{-2}$  for the metal-insulator transition.

The scaling parameters  $B_c$  and  $k_B$  in the analysis by Shashkin et al (2001a) and Vitkalov et al (2001b) represent energy scales  $k_B B_c$  and  $k_B T$ , respectively, which vanish at or near the critical electron density for the metal-insulator transition. At high electron densities and low temperatures  $T < k_B B_c = k_B T$  (corresponding to  $T < T_c$ ), the system is in the zero temperature limit. As one approaches  $n_c$ , progressively lower temperatures are required to reach the zero temperature limit. At  $n_s = n_0$ , the energies  $k_B B_c$  and  $k_B T$  vanish; the parameter  $B_c \rightarrow 0$  as  $T \rightarrow 0$ ; the system thus

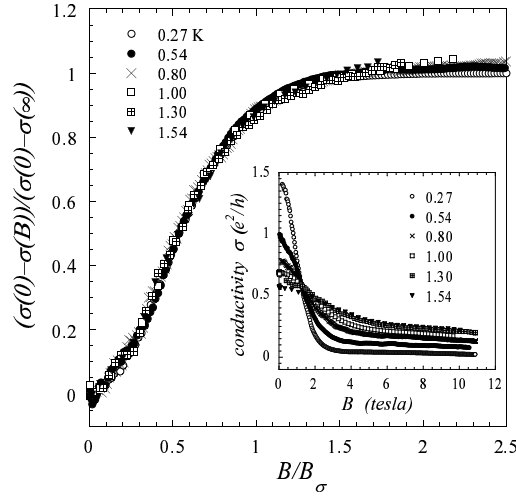


Figure 19. Data collapse obtained by applying the scaling procedure, Eq.2, to the magnetoconductivity at different temperatures for electron density  $n_s = 9.4 \times 10^{10} \text{ cm}^{-2}$ . The inset shows the conductivity at different temperatures as a function of magnetic field. Adopted from Vitkalov et al (2001b).

exhibits critical behaviour (Sondhi et al 1997; Vojta 2003), signalling the approach to a new phase in the limit  $T = 0$  at a critical density  $n_0 = n_c$ .

#### 4. SPIN SUSCEPTIBILITY NEAR THE METAL-INSULATOR TRANSITION

##### 4.1. Experimental measurements of the spin susceptibility

In the Fermi-liquid theory, the electron effective mass and the g-factor (and, therefore, the spin susceptibility  $\chi / g m^*$ ) are renormalized due to electron-electron interactions (Landau 1957). Earlier experiments (Fang and Stiles 1968; Smith and Stiles 1972), performed at relatively small values of  $r_s \approx 2$  to 5, confirmed the expected increase of the spin susceptibility. More recently, Okamoto et al (1999) observed a renormalization of  $\chi$  by a factor of  $\approx 2.5$  at  $r_s$  up to about 6 (see Fig. 24 (a)). At yet lower electron densities, in the vicinity of the metal-insulator transition, Kravchenko et al (2000b) have observed a disappearance of the energy gaps at "cyclotron" filling factors which they interpreted as evidence for an increase of the spin susceptibility by a factor of at least 5.

It was noted many years ago by Stoner that strong interactions can drive an electron system toward a ferromagnetic instability (Stoner 1946). Within some theories of strongly interacting 2D systems (Finkelstein 1983, 1984; Castellani et al 1984), a tendency towards ferromagnetism is expected to accompany metallic behaviour. The experiments discussed in Section 3.2 which indicate that  $B_c$  and  $\nu_c$  vanish at a finite density prompted Shashkin et al (2001a) and Vitkalov et al (2001b) to suggest that spontaneous spin polarization may indeed occur at or near the critical electron density in the limit  $T = 0$ . The data obtained in these experiments provide information from which the spin susceptibility,  $\chi$ , can be calculated in a wide range of

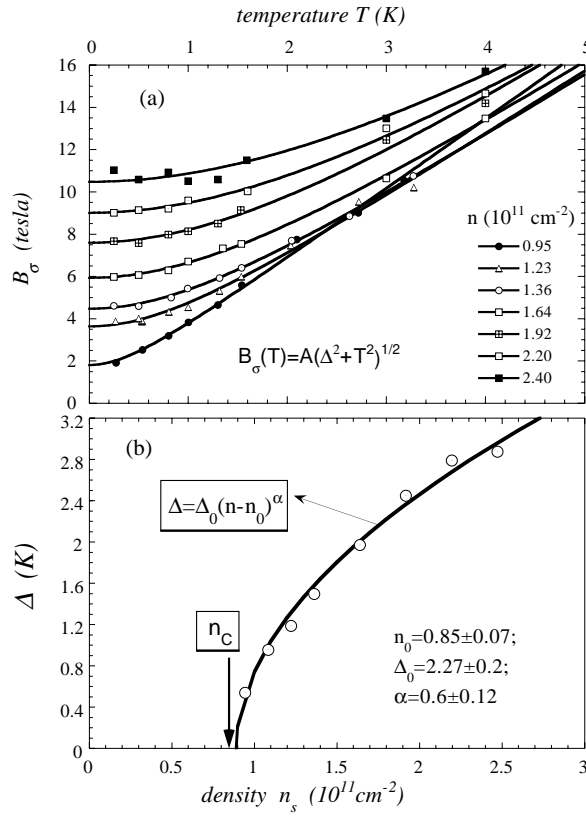


Figure 20. (a)  $B_{\sigma}$  versus temperature for different electron densities; the solid lines are fits to the empirical form  $B_{\sigma}(n_s; T) = A(n_s)[(n_s)^2 + T^2]^{1/2}$ . (b) The parameter  $\Delta$  as a function of electron density; the solid line is a fit to the critical form  $\Delta = \Delta_0(n_s - n_0)^{\alpha}$ . From Vitkalov et al (2001b).

densities. In the clean limit, the band tails are small (Vitkalov et al 2002; Dolgoplov and Gold 2002; Gold and Dolgoplov 2002) and can be neglected, and the magnetic field required to fully polarize the spins is related to the  $g$ -factor and the effective mass by the equation  $g \mu_B B_C = 2E_F = \hbar^2 n_s / m$  (here, the two-fold valley degeneracy in silicon has been taken into account). Therefore, the spin susceptibility, normalized by its "non-interacting" value, can be calculated as

$$\frac{\chi}{\chi_0} = \frac{g \mu_B}{g_0 \mu_B} = \frac{\hbar^2 n_s}{2 \mu_B m_b}$$

Fig. 21 shows the normalized spin susceptibility (Shashkin et al 2001a) and its inverse (Vitkalov et al 2002) obtained using the above expression. The values deduced by both groups indicate that  $g \mu_B$  diverges ( $(g \mu_B)^{-1}$  extrapolates to zero) in silicon MOSFETs at a finite density close or equal to  $n_c$ . Also shown on the same figure are the data of Pudalov et al obtained from an analysis of Shubnikov-de Haas (SdH) measurements in crossed magnetic fields (see section 4.2). The susceptibilities obtained by all three groups on different samples, by different methods and in different ranges of magnetic field, are remarkably similar (on the mutual consistency of the data obtained

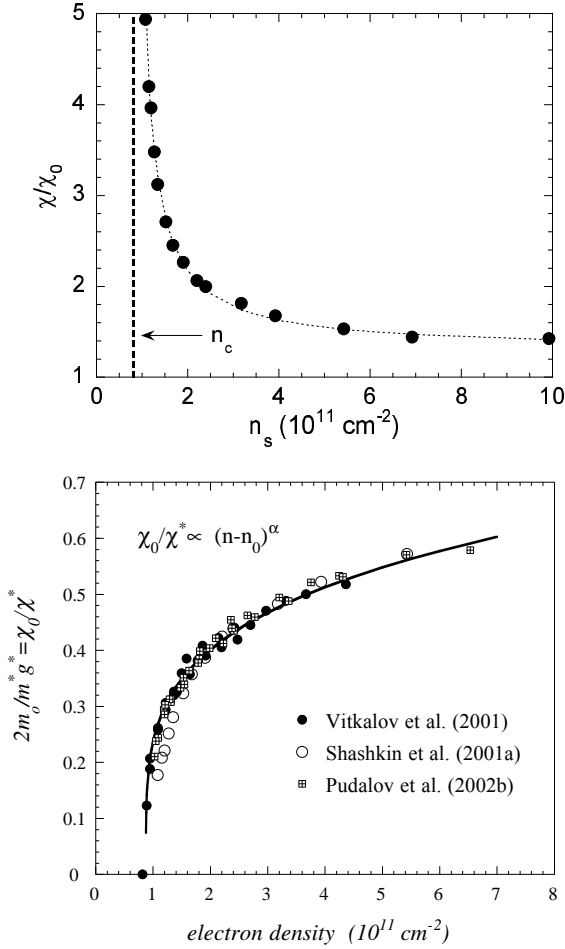


Figure 21. Upper graph: normalized spin susceptibility vs  $n_s$  obtained from the data in Fig. 17. The dashed line is a guide to the eye. The vertical dashed line denotes the position of the critical density for the metal-insulator transition. Lower graph: the inverse of the normalized spin susceptibility  $\chi_0^* =$  versus electron density obtained by Vitkalov et al. (2001b), plotted with data of Shashkin et al. (2001a) and Pudalov et al. (2002b). The solid curve is a fit to the critical form  $\chi_0^* = A(n_s - n_0)^\alpha$  for the data of Vitkalov et al. (2001b) (excluding the point shown at  $\chi_0^* = 0$ ). Adapted from Vitkalov et al. (2002).

on different samples by different groups, see also Kravchenko et al. (2002) and Sarachik and Vitkalov (2003)).

A novel and very promising method has recently been used by Purus et al. (2003) to obtain direct measurements of the thermodynamic spin susceptibility. The method entails modulating the (parallel) magnetic field by an auxiliary coil and measuring the AC current induced between the gate and the 2D electron gas, which is proportional to  $\partial \mu / \partial B$  (where  $\mu$  is the chemical potential). Using Maxwell's relation,

$$\frac{\partial \mu}{\partial B} = \frac{\partial M}{\partial n_s};$$

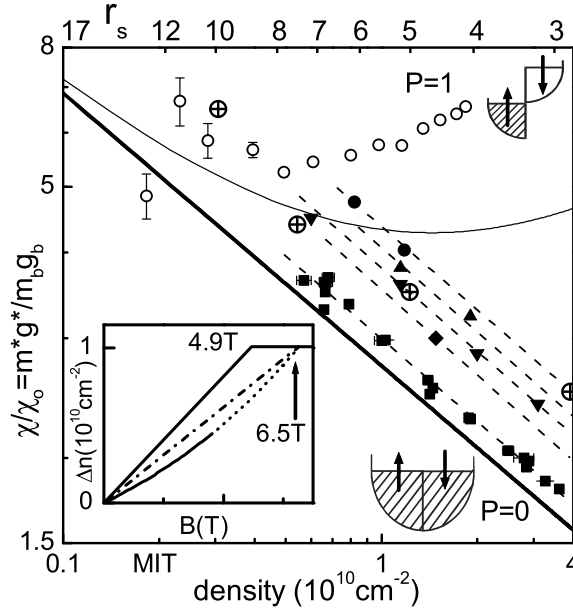


Figure 22. Density-dependence of  $m^*g^*$  in an ultra-clean 2D electron system in GaAs/AlGaAs determined by two different methods. The solid data points are obtained from tilted-field Shubnikov-de Haas measurements with different configurations of Landau levels. The parallel dashed lines indicate a power law dependence of  $m^*g^*$  with a single exponent for all level configurations. The open circles show nonmonotonic density-dependence of  $m^*g^*$  derived from the full-polarization field,  $B_c$ , using the parallel field method. The inset shows the net spin for  $n_s = 1 \times 10^{10} \text{ cm}^{-2}$  with interpolated regime (solid line) and extrapolated regime (dotted line).  $B_c = 4.9 \text{ T}$  from the in-plane field method and  $B_{ext} = 6.5 \text{ T}$  from extrapolation of the tilted-field method. The thick solid line represents extrapolation of  $m^*g^*$  to the  $P=0$  limit. Calculations from Attacalite et al (2002) are shown as crossed circles. Adapted from Zhu et al (2003).

one can obtain the magnetization  $M$  by integrating the induced current over  $n_s$ . The magnetic susceptibility can then be determined from the slope of the  $M(B)$  versus  $B$  dependence at small fields. To date, Pirus et al have reported data for one sample which becomes insulating at a relatively high electron density ( $1.3 \times 10^{10} \text{ cm}^{-2}$ ), and the data obtained below this density are irrelevant for the metallic regime we are interested in. For this reason, the data collected so far do not provide information about the most interesting regime just above  $n_c$ .

In GaAs/AlGaAs heterostructures, a similar strong increase of the spin susceptibility at ultra-low carrier densities has now been established based on an analysis of the Shubnikov-de Haas oscillations (Zhu et al 2003). The results are shown in Fig. 22 by solid symbols;  $\chi/\chi_0$  increases by more than a factor of two as the density decreases. Zhu et al suggested an empirical equation  $\chi/\chi_0 \propto n_s^{-0.4}$  to describe their experimental data, which works well in the entire range of electron densities spanned. Although  $\chi/\chi_0$  tends toward a divergence, it is not clear from these experiments whether it does so at a finite density. We note that due to the lower effective mass, higher dielectric constant and the absence of valley degeneracy, the ratio  $r$  between Coulomb and Fermi energies in GaAs/AlGaAs is an order of magnitude smaller than

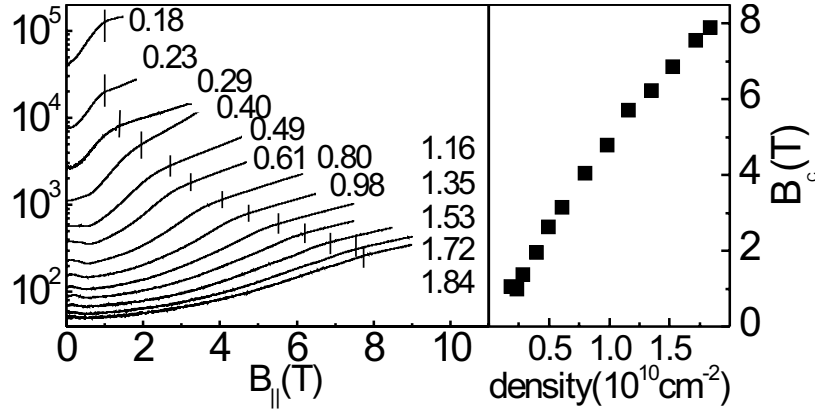


Figure 23. Left hand panel: magnetoresistance of GaAs/AlGaAs as a function of in parallel field for different electron densities indicated in unit of  $10^{10} \text{ cm}^{-2}$ ; the positions of the magnetic fields,  $B_c$ , required for full polarization are indicated following Tutuc et al (2002). Right hand panel:  $B_c$  as a function of density. Adopted from Zhu et al (2003).

in silicon MOSFETs at the same electron density; therefore, to reach the same relative interaction strength, samples are required which remain metallic at densities about two orders of magnitude lower than in silicon, i.e.,  $< 10^9 \text{ cm}^{-2}$ . The currently accessible electron densities in GaAs/AlGaAs heterostructures are still too high to reliably establish the limiting behaviour of  $\chi$ .

The open circles in Fig. 22 denote  $\chi(n_s)$  derived from an alternative method for measuring  $B_c$  based on a determination of the parallel magnetic field corresponding to the "knee" of the magnetoresistance curves, as shown in the left hand panel of Fig. 23. Earlier, this method yielded an anomalous and quite puzzling decrease of the susceptibility with decreasing density in both hole (Tutuc et al 2002) and electron (Noh et al 2002) systems in GaAs/AlGaAs. This was in disagreement with findings in Si MOSFETs, and argued against any spontaneous spin polarization. These results are now believed to be in error for a number of possible reasons. The field for full spin polarization, marked by vertical bars in Fig. 23 (left hand panel) and plotted as a function of  $n_s$  in Fig. 23 (right hand panel), decreases with decreasing carrier density and exhibits an apparent saturation below  $n_s = 0.23 \times 10^{10} \text{ cm}^{-2}$ . Calculation based on this saturation field would yield a spin susceptibility that decreases below this density. However, the saturation field may be constant below this density due to the fact that the experiments are performed at a temperature which is too high; if the temperature were decreased further, the saturation field would probably continue to decrease, consistent with the decrease of  $B_c$  shown in Fig. 20 (a). Another possible source of error is the finite thickness of the electron layer in GaAs/AlGaAs heterostructures, which leads to an increase in the effective mass with increasing parallel magnetic field (Batke and Tu 1986). Indeed, it has recently been shown by Zhu et al (2003) that the conclusion that the spin susceptibility decreases with decreasing carrier density is erroneous and originates from the fact that the effective mass depends on magnetic field. The effect of the finite thickness on the spin susceptibility was studied in detail by Tutuc et al (2003).

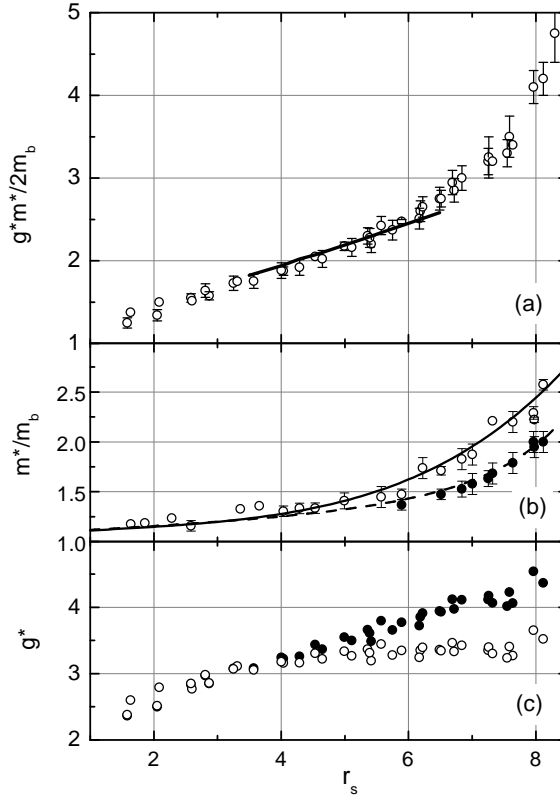


Figure 24. The parameters  $g^*$ ,  $m^*$ , and  $g^*m^*/2m_b$  for different silicon samples as a function of  $r_s$  (dots). The solid line in (a) shows the data of Okamoto et al (1999). The solid and open dots (b) and (c) correspond to two different methods of finding  $m^*$  (see the text). The solid and dashed lines in (b) are polynomial fits for the two functions for  $m^*$  ( $r_s$ ). Adapted from Pudalov et al (2002).

#### 4.2. Effective mass and g-factor

In principle, the increase of the spin susceptibility could be due to an enhancement of either  $g$  or  $m^*$  (or both). To obtain  $g$  and  $m^*$  separately, Pudalov et al (2002b) performed measurements of SdH oscillations in superimposed and independently controlled parallel and perpendicular magnetic fields. Their results are shown in Fig. 24. The data were taken at relatively high temperatures (above 300 mK), where the low- $n_s$  resistance depends strongly on temperature. Therefore, the conventional procedure of calculating the effective mass from the temperature dependence of the amplitude of the SdH oscillations is unreliable, as it assumes a temperature-independent Dirigle temperature. Pudalov et al considered two limiting cases: a temperature-independent  $T_D$ , and a  $T_D$  that linearly increases with temperature; two sets of data based on these assumptions are plotted in Fig. 24 (b) and (c). Within the uncertainty associated with the use of these two methods, both  $g$  and  $m^*$  were found to increase with decreasing  $n_s$ .

Shashkin et al (2002) used an alternative method to obtain  $g$  and  $m^*$  separately. They analyzed the data for the temperature dependence of the conductivity in zero magnetic field using the recent theory of Zala et al (2001). According to this theory,

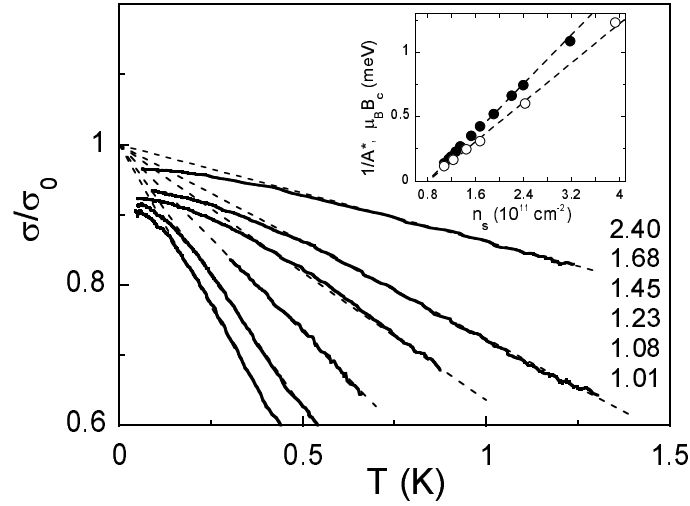


Figure 25. For a low-disordered silicon MOSFET, the temperature dependence of the normalized conductivity at different electron densities (indicated in units of  $10^{11} \text{ cm}^{-2}$ ) above the critical electron density for the metal-insulator transition. The dashed lines are fits to the linear portions of the curves. The inset shows  $1/A^*$  ( $n_s$ ) (see Eq. 3) and  $B_c(n_s)$  (open and solid circles, respectively). The dashed lines are continuations of the linear fits, which extrapolate to the critical electron density for the metal-insulator transition. From Shashkin et al (2002).

is a linear function of temperature:

$$\frac{\sigma(T)}{\sigma_0} = 1 - A k_B T; \quad (3)$$

where the slope,  $A$ , is determined by the interaction-related parameters: the Fermi liquid constants  $F_0^a$  and  $F_1^s$ :

$$A = \frac{(1 + 8F_0^a)g m}{h^2 n_s}; \quad \frac{g}{g_0} = \frac{1}{1 + F_0^a}; \quad \frac{m}{m_b} = 1 + F_1^s \quad (4)$$

(here  $g_0 = 2$  is the "bare"  $g$ -factor.) These relations allow a determination of the many-body enhanced  $g$  factor and mass  $m$  separately using the data for the slope  $A$  and the product  $g m$ .

The dependence of the normalized conductivity on temperature,  $\sigma(T)/\sigma_0$ , is displayed in Fig. 25 at different electron densities above  $n_c$ ; the value of  $\sigma_0$  used to normalize  $\sigma$  was obtained by extrapolating the linear interval of the  $\sigma(T)$  curve to  $T = 0$ . The inverse slope  $1/A^*$  (open circles) and  $B_c(n_s)$  (solid circles) are plotted as a function of  $n_s$  in the inset to Fig. 25. Over a wide range of electron densities,  $1/A^*$  and  $B_c$  are close to each other; the low-density data for  $1/A^*$  are approximated well by a linear dependence which extrapolates to the critical electron density  $n_c$  in a way similar to  $B_c$ .

Values of  $g = g_0$  and  $m = m_b$  determined from this analysis are shown as a function of the electron density in Fig. 26. In the high  $n_s$  region (relatively weak interactions), the enhancement of both  $g$  and  $m$  is relatively small, both values increasing slightly with decreasing electron density in agreement with earlier data (Ando et al 1982). Also, the renormalization of the  $g$ -factor is dominant compared to that of the effective

mass, consistent with theoretical studies (Iwamoto 1991; Kwon et al 1994; Chen and Raikh 1999). In contrast, the renormalization at low  $n_s$  (near the critical region), where  $r_s \gg 1$ , is much more striking. As the electron density is decreased, the

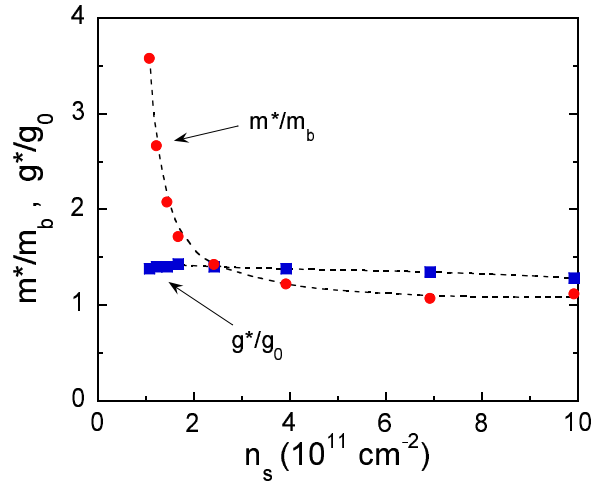


Figure 26. The effective mass (circles) and  $g$  factor (squares) in a silicon MOSFET, determined from the analysis of the parallel field magnetoresistance and temperature-dependent conductivity, versus electron density. The dashed lines are guides to the eye. From Shashkin et al (2002).

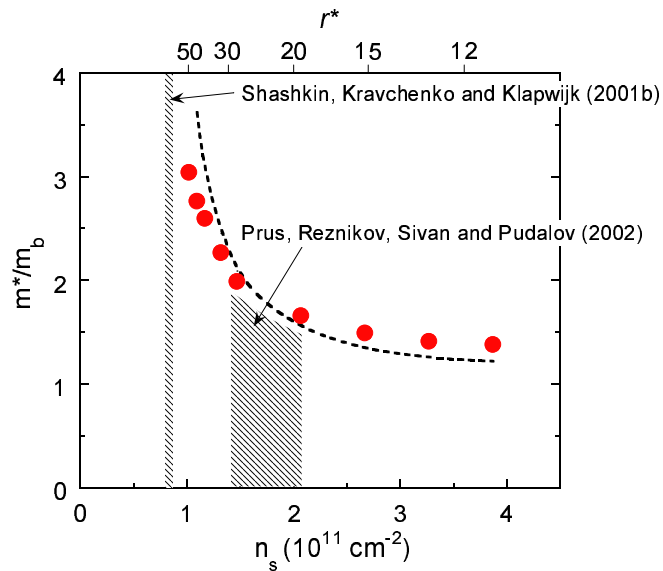


Figure 27. For a silicon MOSFET, the effective mass obtained from an analysis of  $(B_k)$  (dotted line) and from an analysis of SdH oscillations (circles). Data of Shashkin et al (2003a). The upper x-axis shows  $r^*$  calculated using the latter value for the effective mass. The shaded areas correspond to metallic regimes studied in papers by Shashkin et al (2001b) and Prus et al (2002), as labelled.

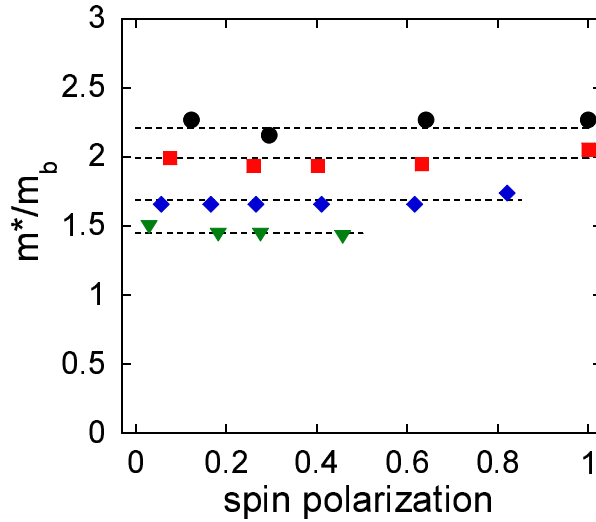


Figure 28. For silicon MOSFETs, the effective mass versus the degree of spin polarization for the following electron densities in units of  $10^{11} \text{ cm}^{-2}$ : 1.32 (dots), 1.47 (squares), 2.07 (diamonds), and 2.67 (triangles). The dashed lines are guides to the eye. From Shashkin et al (2003a).

renormalization of the effective mass increases markedly with decreasing density while the g factor remains relatively constant. Hence, this analysis indicates that it is the effective mass, rather than the g-factor, that is responsible for the strongly enhanced spin susceptibility near the metal-insulator transition. To verify this conclusion, Shashkin et al (2003a, 2003b) used an independent method to determine the effective mass through an analysis of the temperature dependence of the SdH oscillations similar to the analysis done by Smith and Stiles (1972) and Pudalov et al (2002b), but extended to much lower temperatures where the Dingle temperature is expected to be constant and the analysis reliable. In Fig. 27, the effective mass obtained by this method is compared with the results obtained by the procedure described above (the dotted line). The quantitative agreement between the results obtained by two independent methods supports the validity of both. The data for the effective mass are also consistent with data for spin and cyclotron gaps obtained by magnetocapacitance spectroscopy (Khrapai et al 2003).

To probe a possible connection between the effective mass enhancement and spin and exchange effects, Shashkin et al (2003a, 2003b) introduced a parallel magnetic field component to align the electrons' spins. In Fig. 28, the effective mass is shown as a function of the spin polarization,  $P = (B_z^2 + B_k^2)^{1/2} = B_c$ . Within the experimental accuracy, the effective mass does not depend on  $P$ . Therefore, the enhancement of  $m^*$  near the MIT is robust, and the origin of the mass enhancement has no relation to the electrons' spins and exchange effects.

#### 4.3. Electron-electron interactions near the transition

The interaction parameter,  $r_s = E_C/E_F$ , is generally assumed to be equal to the dimensionless Wigner-Seitz radius,  $r_s = 1/(n_s)^{1/2} a_B$ , and, hence, proportional to

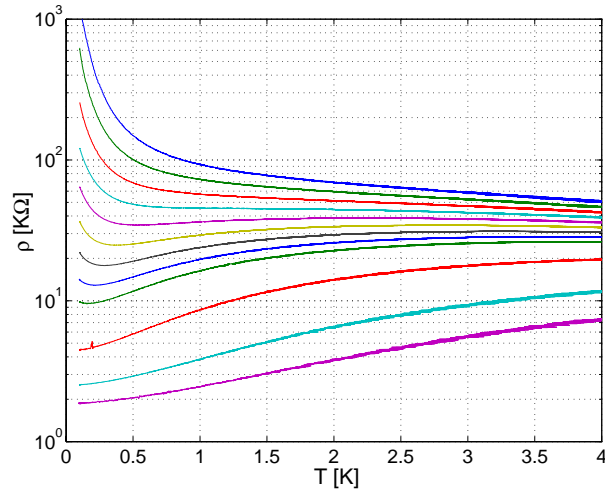


Figure 29.  $\rho(T)$  in a moderately disordered silicon MOSFET. Densities from top to bottom are  $n_s = 1.20$  to  $1.44$  (in  $0.03$  steps),  $1.56$ ,  $1.8$  and  $2.04 \times 10^{11} \text{ cm}^{-2}$ . From Pirus et al (2002).

$n_s^{-1/2}$ . However, this is true only if the effective mass does not depend on  $n_s$ ; close to the transition, where the effective mass is strongly enhanced, the deviations from the square root law become important, and the interaction parameter is larger than the Wigner-Seitz radius by a factor of  $m^* = m_b$  (or  $2m^* = m_b$  in silicon MOSFETs, where an additional factor of 2 derives from the valley degeneracy).

Near the metal-insulator transition,  $r$  grows rapidly due to the sharp increase of the effective mass, as shown on the upper x-axis in figure 27; here  $r$  is calculated using the effective mass obtained from the analysis of the SdH oscillations. We note that since at low  $n_s$  this method yields a somewhat smaller effective mass than the method based on the analysis of  $\rho(B_k)$ , the plotted values represent the most conservative estimate for  $r$ . Due to the rapid increase of  $m^*$  near the transition, even small changes in the electron density may lead to large changes in  $r$ . For example, the transition to a localized state in a low-disordered sample used by Shashkin et al (2001b) occurs at  $n_s = 0.795 \times 10^{11} \text{ cm}^{-2}$  (see Fig. 15), while in a sample of lesser quality used by Pirus et al (2002), it occurs at  $1.44 \times 10^{11} \text{ cm}^{-2}$  (see Fig. 29). The areas corresponding to the metallic regimes studied in these papers are shaded in Fig. 27; the corresponding values of  $r$  differ dramatically (the actual values of  $r$  in the study by Shashkin et al are not known because the effective mass has not been determined near the transition; the lower boundary for  $r$  is 50). The difference in  $r$  may account for the qualitative change in the behaviour of the resistance in the two samples: in the more disordered sample, there is no temperature-independent curve (the separatrix), and some of the curves which look "metallic" at higher temperature are insulating below a few hundred mK, suggesting that localization becomes dominant in this sample as  $T \rightarrow 0$ .

## 5. HOW DOES ALL THIS FIT THEORY?

The possibility that a  $B = 0$  metallic state in 2D can be stabilized by interactions was first suggested by Finkelstein (1983, 1984) and Castellani et al (1984). In this

theory, the combined effects of disorder and interactions were studied by perturbative renormalization group methods. It was found that as the temperature is decreased, the resistivity increases and then decreases at lower temperatures, suggesting that the system is approaching a low-temperature metallic state. An external magnetic field, via Zeeman splitting, drives the system back to the insulating state. These predictions of the theory are in qualitative agreement with experiments.

However, an interaction parameter scales to infinitely large values before zero temperature is reached, and the theory thus becomes uncontrolled; this scenario has consequently not received general acceptance. It should also be noted that the theory may not be applicable to the current experiments since it was developed for the diffusive regime:  $T \ll \hbar = v_F^2 \tau$ , where  $\tau$  is the elastic mean-free time extracted from the Drude conductivity (Boltzmann constant is assumed to be equal to 1 throughout this section). This condition corresponds to the low-temperature limit  $T \ll T_F = (\hbar/e^2)$ . Since the Fermi temperature,  $T_F$ , is rather low at the small carrier densities considered here, the above condition is satisfied only close to the transition, where  $\tau$  becomes of the order of  $\hbar/e^2$ . In the experiments, however, the characteristic decrease of the resistance with decreasing temperature often persists into the relatively high-temperature ballistic regime  $T > \hbar = v_F^2 \tau$  (or  $T > T_F = (\hbar/e^2)$ ). Altshuler et al (2001) and Brunthaler et al (2001) have interpreted this observation as evidence that the mechanism responsible for the strong temperature dependence cannot originate from quantum interference.

For the ballistic region, calculations in the random phase approximation were carried out two decades ago by Stern (1980), Gold and Dolgoplov (1986), Das Sarma (1986) and were recently refined by Das Sarma and Hwang (1999). These theories predict a linear temperature dependence for the conductivity with metallic-like slope ( $d\sigma/dT < 0$ ) regardless of the strength of the interactions. The spin degree of freedom is not important in this theory and enters only through the Fermi energy, which is a factor of two larger for the spin-polarized than for the unpolarized system. Therefore, the application of a (parallel) magnetic field does not eliminate the metallic temperature dependence.

The two limits | diffusive and ballistic | had until recently been assumed to be governed by different physical processes. However, Zala et al (2001) have shown that the temperature dependence of the conductivity in the ballistic regime originates from the same physical process as the Altshuler-Aronov-Lee corrections: coherent scattering of electrons by Friedel oscillations. In this regime the correction is linear in temperature, as is the case for the results mentioned in the previous paragraph. However, the value and even the sign of the slope depends on the strength of electron-electron interaction, the slope being directly related to the renormalization of the spin susceptibility (see also Gold 2001, 2003). By aligning the spins, a magnetic field causes a positive magnetoresistance and changes the temperature dependence of the conductivity from metallic-like to insulating-like (Herbut 2001; Zala et al 2002; Gold 2003), in agreement with experiments.

### 5.1. The diffusive regime: Renormalization group analysis

It is well known that in the diffusive limit ( $T \ll \hbar$ ), electron-electron interactions in two dimensional disordered systems lead to logarithmically divergent corrections to

the conductivity given by:

$$\sigma = \frac{e^2}{2\pi^2 h} \ln \frac{h}{T} \left[ 1 + \frac{3}{2} \frac{\ln(1 + F_0)}{F_0} \right]; \quad (5)$$

where  $F_0$  is the interaction constant in the triplet channel which depends on the interaction strength. The sign of this logarithmically divergent correction may be positive (metallic-like) or negative (insulating-like), depending on the value of  $F_0$ .

Experimentally, the diffusive regime is realized in a relatively narrow range of electron densities near the metal-insulator transition, where the resistivity is of the order of  $h/e^2$ . Punnoose and Finkelstein (2002) have convincingly demonstrated that in this region, the temperature dependence of the resistivity can be understood within the renormalization group theory describing the effect of the electron-electron interactions on the propagation of diffusive collective modes, with the delocalizing component becoming dominant in dilute 2D systems.

In 2D, the renormalization group equation describing the evolution of the resistivity has been derived previously by Finkelstein:

$$\frac{dg}{d} = g^2 \left[ 1 + \frac{3}{2} \frac{1 + \alpha}{2} \ln(1 + \alpha) \right]; \quad (6)$$

Here  $g = \ln(T/h)$ , the dimensionless parameter  $g$  is the conductance in units of  $e^2/h$  and  $\alpha$  is the coupling constant. The first term in the square brackets of Eq. 6 corresponds to the weak localization correction (quantum interference; Abraham et al 1979), while the second term is the contribution of the singlet density mode which is due to the long range nature of the Coulomb interaction (Altshuler, Aronov and Lee 1980). The last term describes the contribution of the three triplet modes. Note that the last two terms have opposite signs, favouring localization and delocalization, respectively. The resulting dependence  $g(\alpha)$  becomes delocalizing when  $\alpha > \alpha_c = 2.04$ . This requires the presence of rather strong electron correlations.

In the case of two distinct valleys (as in (100) silicon MOSFETs), Eq. 6 can be easily generalized to:

$$\frac{dg}{d} = g^2 \left[ 2 + \frac{15}{2} \frac{1 + \alpha}{2} \ln(1 + \alpha) \right]; \quad (7)$$

The difference between the numerical factors in Eq. 6 and Eq. 7 results from the number of degrees of freedom in each case. The weak localization term becomes twice as large. The difference in the number of the multiplet modes increases the coefficient of the  $\alpha$  term from 3 to 15. As a result of these modifications, the value of  $\alpha_c$  required for the dependence  $g(\alpha)$  to become delocalizing is reduced to  $\alpha_c = 0.45$ ; which makes it easier in the case of two valleys to reach the condition where the resistivity decreases with decreasing temperature.

In conventional conductors the initial values of  $\alpha$  are small, and the net effect is in favour of localization. In dilute systems, however, this value is enhanced due to electron-electron correlations. In addition,  $\alpha$  also experiences logarithmic corrections due to the disorder (Finkelstein 1983, 1984; Castellani et al 1984, 1998). The equation describing the renormalization group evolution of  $\alpha$  is the same for the case of one and two valleys:

$$\frac{d\alpha}{d} = g \frac{(1 + \alpha)^2}{2}; \quad (8)$$

It follows from this equation that  $\alpha$  increases monotonically as the temperature is decreased. Once it exceeds  $\alpha_c$ , the resistivity passes through a maximum. Even though

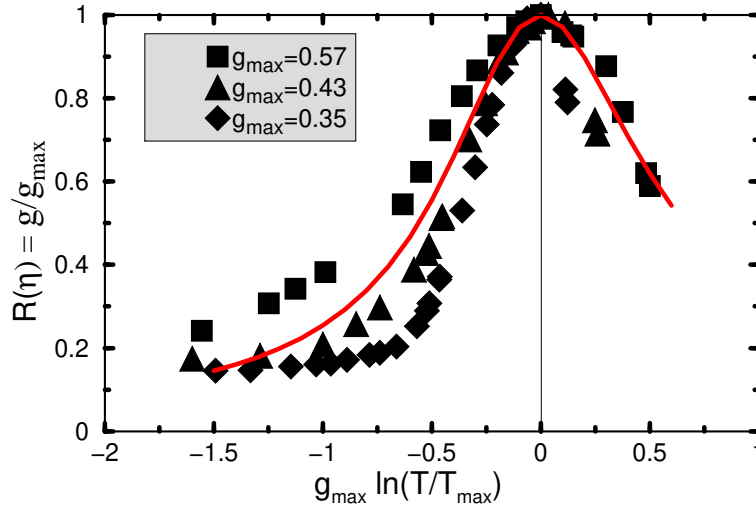


Figure 30. Data for silicon MOSFETs at  $n_s = 0.83, 0.88$  and  $0.94 \times 10^{11} \text{ cm}^{-2}$  from Pudalov et al (1998) are scaled according to Eq. 9. The solid line corresponds to the solution of the renormalization group, Eqs. 7 and 8; no adjustable parameters were used in this fit. From Punnoose and Finkelstein (2002).

the initial values of  $g$  and  $g_2$  are not universal, the flow of  $g$  can be described by a universal function  $R(\eta)$  (Finkelstein, 1983):

$$g = g_{\text{max}} R(\eta) \quad \text{and} \quad \eta = g_{\text{max}} \ln(T_{\text{max}}/T); \quad (9)$$

where  $T_{\text{max}}$  is the temperature at which  $g$  reaches its maximum value  $g_{\text{max}}$ .

In Fig. 30, the theoretical calculations are compared with the experimental data obtained by Pudalov et al (1998). Since the renormalization group equations were derived in the lowest order in  $g$  and cannot be applied in the critical region where  $g > 1$ , only curves with maximum  $g$  ranging from  $g_{\text{max}} = 0.3$  to  $g_{\text{max}} = 0.6$  are shown in the figure. The decrease in the resistivity by up to a factor of five, as well as its saturation, are both captured in the correct temperature interval by this analysis without any adjustable parameters.

In agreement with experiment, this universal behaviour can be observed only in ultra clean samples (with negligible inter-valley scattering) and will not be found in samples that are only moderately clean. In disordered silicon MOSFETs, a description in terms of an effective single valley is relevant, and the large value of  $\alpha_2 = 2.04$  makes it difficult for the non-monotonic  $\rho(T)$  to be observed as the initial values of  $g_2$  are usually much less than 2.04. As a result, for  $g$  near the critical region, the resistivity becomes insulating-like instead of going through the maximum.

Therefore, in ultra clean silicon MOSFETs, the behaviour of the resistivity not far from the transition is quantitatively well described by the renormalization group analysis that considers the interplay of the electron-electron interactions and disorder when the electron band has two distinct valleys. The theory in this case remains in control down to exponentially low temperatures, unlike the single valley case, where  $g_2$  diverges at  $g = 1$ , or at temperatures just below  $T_{\text{max}}$ . A parallel magnetic field provides a Zeeman splitting and gives rise to positive magnetoresistance (Lee

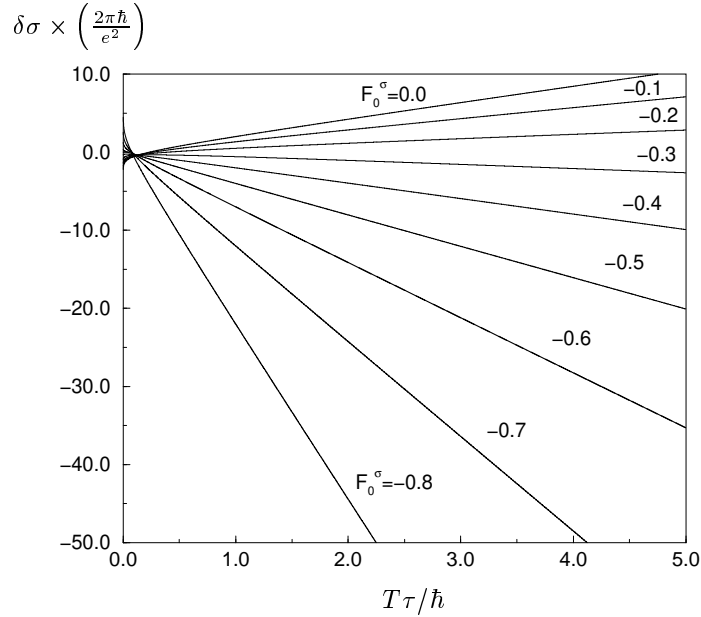


Figure 31. Total interaction correction to the conductivity. The curve for  $F_0 = 0$  corresponds to the universal behaviour of a completely spin polarized electron gas. From Zala et al (2001).

and Ramakrishnan 1982; Finkelstein 1984; Castellani et al 1998). In a very strong magnetic field, when the electrons are completely spin-polarized, the system becomes "spinless". In this case, the system always scales to an insulator, and in the weak disorder limit, a universal logarithmic temperature dependence is expected:

$$\sigma(T) = \sigma_0 + (e^2/h) (2 - 2 \ln 2) \ln(T/\hbar):$$

5.2. Farther from the transition (the ballistic regime)

Far from the transition ( $n_s \gg n_c$ ), the inverse scattering time  $\tau^{-1}$  is often smaller than the temperature at which the experiments are performed, and one is in the ballistic regime:  $T \ll \hbar$ . The interaction theory by Zala et al (2001) considers coherent electron scattering on the Friedel oscillations. The phase of the Friedel oscillation is such that the wave scattered from the impurity interferes constructively with the wave scattered from the oscillation, leading to a quantum correction to the Drude conductivity,  $\sigma_0$ . As has already been mentioned, this correction ( $\sigma_0$ ), which is logarithmic in the diffusive regime, becomes linear in the ballistic regime:

$$\sigma(T) = \frac{e^2}{h} \frac{T}{\hbar} \left( 1 + \frac{3F_0}{1 + F_0} \right) = \sigma_0 \left( 1 + \frac{3F_0}{1 + F_0} \frac{T}{T_F} \right) \quad (10)$$

where  $F_0$  is the Fermi liquid interaction parameter in the triplet channel. As in the diffusive regime, the sign of  $d\sigma/dT$  depends on the constant  $F_0$ .

The total correction to the conductivity is shown in Fig. 31 for different values of  $F_0$ . The divergence at low temperature is due to the usual logarithmic correction (Altshuler, Aronov and Lee 1980; Finkelstein 1983, 1984; Castellani et al 1984).

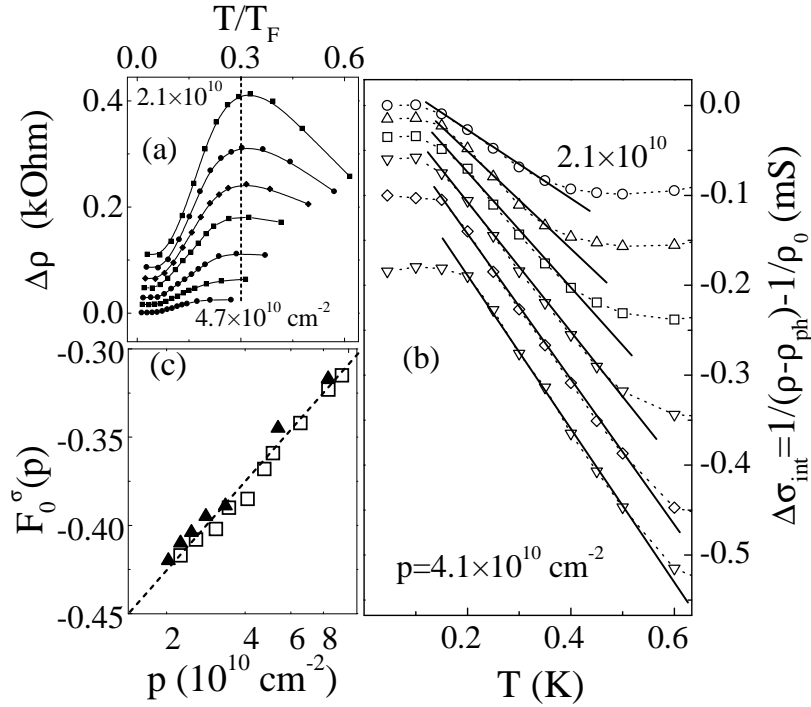


Figure 32. (a)  $\Delta\rho$  as a function of the dimensionless temperature ( $T=T_F$ ) at different  $p$  in a p-type GaAs/AlGaAs heterostructure. (For clarity, curves in (a) and (b) are offset vertically.) (b) The same data as in (a) plotted as conductivity, with linear fits. (c) Fermi liquid parameter versus hole density. Open symbols show the result obtained from the analysis of  $\Delta\rho(T)$  at zero magnetic field; closed symbols show results obtained from the parallel-field magnetoresistance. From Proskuryakov et al (2002).

Although the exact value of  $F_0$  cannot be calculated theoretically (in particular, its relation to the conventional measure of the interaction strength,  $r_s$ , is unknown for  $r_s > 1$ ), it can in principle be found from a measurement of the Pauli spin susceptibility. The correction to the conductivity is almost always monotonic, except for a narrow region  $0.45 < F_0 < 0.25$ .

As in the diffusive limit, magnetic field in the ballistic regime suppresses the correction in the triplet channel in Eq. (10), resulting in a universal, positive correction to the Drude conductivity in magnetic field,  $B_0^B$ , and hence in the insulating-like behaviour of  $\Delta\rho(T)$ :

$$= \frac{B_0^B}{T_F} \text{ at } B = B_s; \tag{11}$$

where  $B_s$  is the field corresponding to full spin polarization of the 2D system.

Proskuryakov et al (2002) were the first to perform a quantitative comparison of experimental data (obtained on p-type GaAs/AlGaAs) with the above theory. Their data for the temperature-induced corrections to the conductivity are plotted in Fig. 32 (b). (To extract corrections to the conductivity, Proskuryakov et al used

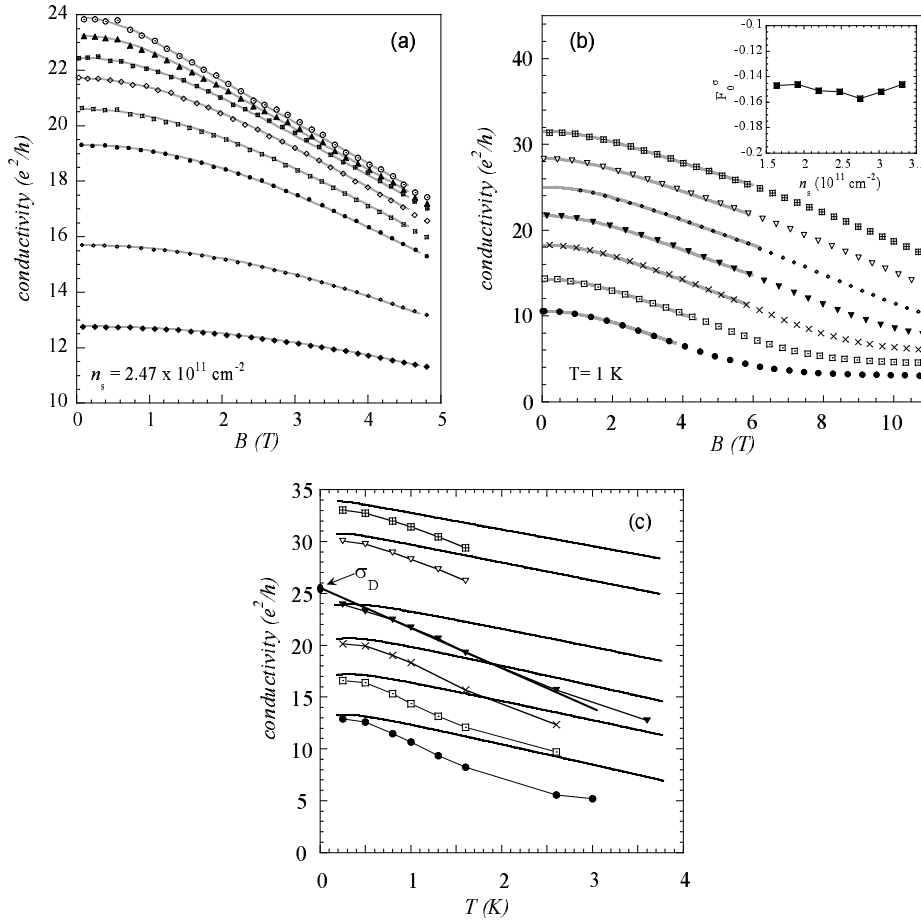


Figure 33. For parameters  $T = 1 \text{ K}$  and  $F_0 = 0.15$ , the magnetoconductivity of a silicon MOSFET: (a) For different temperatures at a fixed density  $n_s = 2.47 \times 10^{11} \text{ cm}^{-2}$ ;  $T = 0.25, 0.5, 0.8, 1.0, 1.3, 1.6, 2.6$  and  $3.6 \text{ K}$  (from top). (b) For different densities at a fixed temperature of  $1 \text{ K}$ ;  $n_s = 3.3, 3.0, 2.75, 2.47, 2.19, 1.92$  and  $1.64 \times 10^{11} \text{ cm}^{-2}$  (from top). (c) The conductivity as a function of temperature for the densities  $n_s = 3.3, 3.0, 2.47, 2.19, 1.92$  and  $1.64 \times 10^{11} \text{ cm}^{-2}$  (from top). Symbols and solid lines denote data and theory, respectively. From Vitkalov et al (2003).

the  $(T)$  dependence shown in Fig. 32 (a) obtained from raw resistivity data by subtracting the contribution of phonon scattering.) A linear fit of  $(T)$  yields the parameter  $F_0$  shown in Fig. 32 (c) for different  $p$ . The interaction constant obtained is negative and provides the metallic slope of  $(T)$ . As expected, the slope increases with decreasing density. When extrapolated to the crossover point from metallic to insulating behaviour ( $p = 1.5 \times 10^{10} \text{ cm}^{-2}$ ), the interaction constant is much higher than the value of  $F_0 = 1$  for the Stoner instability. The transition from metallic-like to insulating-like  $(T)$  in their sample is unlikely to be related to any dramatic change in magnetic properties and is probably caused by Anderson localization.

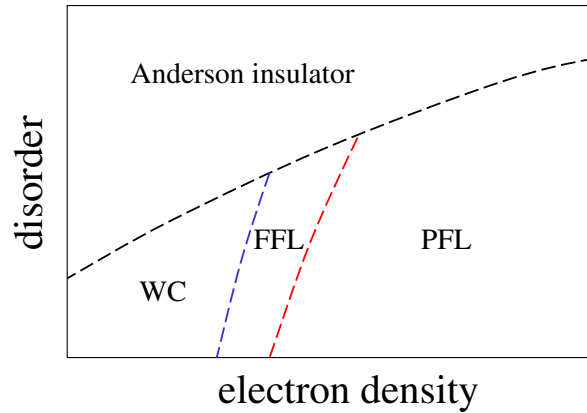


Figure 34. Schematic phase diagram corresponding to the numerical results of Attaccalite et al 2002. The symbols WC, FFL and PFL correspond to the Wigner crystal, ferromagnetic Fermi liquid and paramagnetic Fermi liquid phases, respectively.

Comparison between the experimentally measured  $\rho(T)$  in the ballistic regime with the predictions of Zala et al was also carried out in silicon MOSFETs by Shashkin et al (2002; see sec. 4.2), Vitkalov et al (2003) and Pudalov et al (2003) (see also Das Sarma and Hwang 2003 and Shashkin et al 2003c) and in p-type SiGe heterostructures by Coleridge et al (2002). As shown in Fig. 33 (a) and (b), Vitkalov et al reported quantitative agreement between the theory and their magnetoresistance data in silicon MOSFETs. However, the values of the valley splitting and Fermi liquid parameter  $F_0$  required to obtain fits to the field dependence yield curves that are inconsistent with the observed temperature dependence in zero field, as shown in Fig. 33 (c). This was attributed to the neglect of additional scattering terms that affect the temperature dependence more strongly than the field dependence. Despite this quantitative discrepancy, the theory of Zala et al provides a reasonable description of the conductivity of strongly interacting 2D systems in the ballistic regime.

### 5.3. Approaches not based on Fermi liquid

The calculations of Finkelstein (1983, 1984), Castellani et al (1984) and Zala et al (2001) use the Fermi liquid as a starting point. As discussed earlier,  $r_s$  becomes so large that the theory's applicability is in question near the transition (Chamion et al 2001; for a review, see Vama et al 2002). Moreover, the behaviour of the effective mass reported by Shashkin et al (2003a, 2003b) in the vicinity of the transition is unlikely to be consistent with a Fermi liquid model.

Very little theory has been developed for strongly interacting systems for which  $r_s$  is large but below the expected Wigner crystallization. Several candidates have been suggested for the ground state of the strongly interacting 2D system, among them (i) a Wigner crystal characterized by spatial and spin ordering (Wigner 1934), (ii) an itinerant ferromagnet with spontaneous spin ordering (Stoner 1946), and (iii) a paramagnetic Fermi liquid (Landau 1957). According to numerical simulations (Tanatar and Ceperley 1989), Wigner crystallization is expected in a very dilute

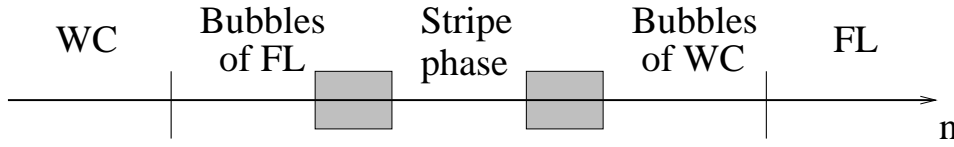


Figure 35. Phase diagram of the 2D electron system at  $T = 0$  suggested by Spivak (2002). The symbols WC and FL correspond to the Wigner crystal and the Fermi liquid phases, respectively. The shaded regions correspond to phases which are more complicated than the bubble and the stripe phases.

regime, when  $r_s$  reaches approximately 35. This value has already been exceeded in the best p-type GaAs/AlGaAs heterostructures; however, no dramatic change in transport properties has occurred at the corresponding density. Recent detailed numerical simulations (Attacalite et al 2002) have predicted that in the range of the interaction parameter  $25 < r_s < 35$  prior to the crystallization, the ground state of the system becomes an itinerant ferromagnet. The corresponding schematic phase diagram is shown in Fig. 34. As discussed earlier, there are experimental indications that a spontaneous spin polarization may occur at a finite electron density in silicon MOSFETs (and possibly in GaAs/AlGaAs heterostructures). Chakravarty et al (1999) have proposed a more complicated phase diagram where the low-density insulating state is a Wigner glass, a phase that has quasi-long-range translational order and competing ferromagnetic and antiferromagnetic spin-exchange interactions. The transition between insulating and metallic states within this theory is the melting of the Wigner glass, where the transition is second order due to the disorder.

Spivak (2002) predicted the existence of an intermediate phase between the Fermi liquid and the Wigner crystal with a first order transition in a clean electron system. The suggested phase diagram is shown in Fig. 35. In analogy with  $\text{He}^3$ , where  $m^*$  increases approaching the crystallization point, Spivak (2001) suggested in an earlier paper that the renormalization of  $m^*$  is dominant compared to that of the  $g$ -factor as the transition is approached, and that  $m^*$  should increase with magnetic field. Although the increase of the mass is in agreement with the experimental results of Shashkin et al (2002, 2003a, 2003b), the suggested increase of  $m^*$  with the degree of spin polarization is not confirmed by their data. The strong increase of the effective mass near crystallization also follows from the approach used by Dolgoplov (2002), who has applied Gutwiler's variational method (Brinkman and Rice 1970) to silicon MOSFETs, and from the dynamical mean-field theory (Tanaskovic et al 2003). However, the predicted dependence of  $m^*$  on the degree of spin polarization is again at odds with the experiment. Dharmawardana (2003) has argued that in two-valley systems, correlation effects outweigh exchange, and a coupled-valley state is formed at  $r_s \approx 5.4$  leading to strong enhancement of the effective mass, which in this case is only weakly dependent on the degree of spin polarization.

## 6. CONCLUSIONS

Significant progress has been achieved during the past few years in understanding the metallic state found a decade ago in strongly interacting 2D systems. There is now considerable evidence that the strong metallic temperature dependence of the resistance in these systems is due to the delocalizing effects of strong electron-

electron interactions. In ultra-clean silicon systems, the temperature dependence of the resistivity is universal near the metal-insulator transition and is quantitatively well described by the renormalization group theory; deep in the metallic state, in the ballistic regime, the temperature dependence of the resistance can be explained by coherent scattering of electrons by Friedel oscillations. In both cases, an external magnetic field quenches the delocalizing effect of interactions by aligning the spins, causing a giant positive magnetoresistance.

The metal-insulator transition is not yet understood theoretically. In silicon MOSFETs, various experimental methods provide evidence for a sharp increase and possible divergence of the spin susceptibility at some finite sample-independent electron density,  $n_c$ , which is at or very near the critical density for the MIT in high mobility samples. Unlike the Stoner instability which entails an increase in the  $g$ -factor, the increase in the susceptibility in these systems is due to an increase of the effective mass. The effective mass is, in turn, found to be independent of the degree of spin polarization, implying that the increase is not due to spin exchange, in disagreement with the Fermi liquid model. A similar increase of the spin susceptibility is observed in GaS/AlGaS heterostructures, but it is not yet clear whether or not it points to a spontaneous spin polarization at a finite carrier density.

The fact that the  $B = 0$  metal-insulator transition in the least disordered silicon samples occurs at or very close to  $n_c$  indicates that the transition in such samples is a property of a clean electron system and is not driven by disorder. Quantum localization appears to be suppressed near the transition in these systems. In lower mobility samples, the localization transition occurs at electron densities much higher than  $n_c$  and may be driven by disorder.

In closing, we note that most of the work done in these dilute two-dimensional systems concerns the transport behaviour, as transport measurements are relatively straightforward (despite problems associated with high impedance electrical contacts at low densities, the need to ensure proper cooling of the electrons system and so on). Studies done to date, many of which are reviewed here, include measurements of the resistivity as a function of temperature and magnetic field, the Hall coefficient, Shubnikov-de Haas oscillations and measurements of noise. Results have also been reported for the compressibility (Dultz and Jiang 2000; Ilani et al 2000, 2001; see also Si and Varna 1998 and Fogler 2003) and capacitive measurements (Khrapai et al 2003) from which one can obtain information about the chemical potential, the density of states, and which provide a measure of the magnetization, as discussed in sec. 4.1.

Many properties that would yield crucial information have not been investigated. Thermodynamic measurements such as specific heat and direct measurements of magnetization would be particularly illuminating; however, these are very difficult, if not impossible, to perform at this time due to the very small number of electrons available in a dilute, two-dimensional layer. Other experiments which could provide valuable information include tunnelling and different resonance techniques. Measurements of one, several, or perhaps all of these may be required for a full understanding of the enigmatic and very interesting behaviour of strongly interacting electrons (or holes) in two dimensions.

Acknowledgments

We are grateful to G B Bachelet, V T Dolgoplov, A M Finkelstein, T M Klapwijk, S Moroni, B N Narozhny, D Neilson, A A Shashkin, C Senatore, B Spivak and S A Vitkalov for useful discussions. SVK is supported by the National Science Foundation grant DMR-0129652 and the Sloan Foundation; MPS is supported by Department of Energy grant no. DE-FG 02-84ER 45153 and National Science Foundation grant DMR-0129581.

## 7. REFERENCES

- Abraham s E, Anderson P W , Licciardello D C and Ram akrishnan T V 1979 Scaling theory of localization: Absence of quantum di usion in two dim ensions Phys. Rev. Lett. 42 673-676
- Abraham s E, K ravchenko S V and Sarachik M P 2001 Metallic behavior and related phenomena in two dim ensions Rev. Mod. Phys. 73 251-266
- Altshuler B L, Aronov A G and Lee P A 1980 Interaction e ects in disordered Ferm i system s in two dim ensions Phys. Rev. Lett. 44 1288-1291
- Altshuler B L and Maslov D L 1999 Theory of metal-insulator transitions in gated sem iconductors Phys. Rev. Lett. 82 145-148
- Altshuler B L, Maslov D L and Pudalov V M 2000 Metal-insulator transition in 2D : Anderson localization in tem perature-dependent disorder? Phys. Status Solidi b 218 193-200
- Altshuler B L, Maslov D L and Pudalov V M 2001 Metal-insulator transition in 2D : resistance in the critical region Physica E 9 209-225
- Ando T, Fowler A B and Stem F 1982 Electronic-properties of two-dim ensional system s Rev. Mod. Phys. 54 437-672
- Attacalite C, Moroni S, Gori-G iorgi P and Bachelet G B 2002 Correlation energy and spin polarization in the 2D electron gas Phys. Rev. Lett. 88 256601
- Batke E and Tu C W 1986 E ective m ass of a space-charge layer on GaAs in a parallelm agnetic- eld Phys. Rev. B 34 3027-3029
- Bishop D J, Tsui D C and Dynes R C 1980 Nonm etallic conduction in electron inversion layers at low tem peratures Phys. Rev. Lett. 44 1153-1156
- Bishop D J, Dynes R C and Tsui D C 1982 M agnetoresistance in Si m etal-oxide-sem iconductor eld-e ect transistors { evidence of weak localization and correlation Phys. Rev. B 26 773-779
- Bogdanovich S and Popovic D 2002 Onset of glassy dynam ics in a two-dim ensional electron system in silicon Phys. Rev. Lett. 88 236401
- Brinkman W F and Rice T M 1970 Application of Gutzwiller's variational m ethod to the m etal-insulator transition Phys. Rev. B 2 4302-4304
- Brunthaler G, Prinz A, Bauer G and Pudalov V M 2001 Exclusion of quantum coherence as the origin of the 2D m etallic state in high-m obility silicon inversion layers Phys. Rev. Lett. 87 096802
- Castellani C, Di Castro C, Lee P A and Ma M 1984 Interaction-driven m etal-insulator transitions in disordered ferm ion system s Phys. Rev. B 30 527-543
- Castellani C, Di Castro C and Lee P A 1998 M etallic phase and m etal-insulator transition in two-dim ensional electronic system s Phys. Rev. B 57 R 9381-R 9384
- Chakravarty S, K ivelson S, Nayak C and Voelker K 1999 W igner glass, spin liquids and the m etal-insulator transition Phil. Mag. B 79 859-868
- Chamon C, M ucciolo E R and Castro Neto A H 2001 P-wave pairing and ferrom agnetism in the m etal-insulator transition in two dim ensions Phys. Rev. B 64 245115
- Chen G-H and Raikh M E 1999 Exchange-induced enhancement of spin-orbit coupling in two-dim ensional electronic system s Phys. Rev. B 60 4826-4833
- Coleridge P T, Williams R L, Feng Y and Zawadzki P 1997 M etal-insulator transition at  $B = 0$  in p-type SiGe Phys. Rev. B 56 R 12764-R 12767
- Coleridge P T, Sachrajda A S and Zawadzki P 2002 W eak localization, interaction e ects, and the m etallic phase in p-SiGe Phys. Rev. B 65 125328
- Das Sarma S 1986 Theory of finite-tem perature screening in a disordered two-dim ensional electron-gas Phys. Rev. B 33 5401-5405
- Das Sarma S and Hwang E H 1999 Charged im purity-scattering-lim ited low-tem perature resistivity of low-density silicon inversion layers Phys. Rev. Lett. 83 164-167
- Das Sarma S and Hwang E H 2000 Parallelm agnetic eld induced giant m agnetoresistance in low density quasi-two-dim ensional layers Phys. Rev. Lett. 84 5596-5599

- Das Sarma S and Hwang E H 2003 On the temperature dependence of 2D "metallic" conductivity in Si inversion layers at intermediate temperatures P reprint cond-m at/0310260
- Dhamawardana M W C 2003 The effective mass and the g-factor of the strongly-correlated 2-D electron fluid: Evidence of a coupled-valley state in the Si system P reprint cond-m at/0307153
- Dobrosavljevic V, Abraham SE, Miranda E and Chakravarty S 1997 Scaling theory of two-dimensional metal-insulator transitions Phys. Rev. Lett. 79 455-458
- Dolan G J and Oshero D D 1979 Nonmetallic conduction in thin metal films at low temperatures Phys. Rev. Lett. 43 721-724
- Dolgoplov V T, Kravchenko G V, Shashkin A A and Kravchenko S V 1992 Properties of electron insulating phase in Si inversion-layers at low temperatures JETP Lett. 55 733-737
- Dolgoplov V T and Gold A 2000 Magnetoresistance of a two-dimensional electron gas in a parallel magnetic field JETP Lett. 71 27-30
- Dolgoplov V T 2002 On effective electron mass of silicon field structures at low electron densities JETP Lett. 76 377-379
- Dolgoplov V T and Gold A 2002 Comment on "Weak anisotropy and disorder dependence of the in-plane magnetoresistance in high-mobility (100) Si-inversion layers" Phys. Rev. Lett. 89 129701
- Dultz S C and Jiang H W 2000 Thermodynamic signature of a two-dimensional metal-insulator transition Phys. Rev. Lett. 84 4689-4692
- Efros A L and Shklovskii B I 1975 Coulomb gap and low temperature conductivity of disordered systems J. Phys. C : Solid State Phys. 8 L49-L51
- Fang F F and Stiles P J 1968 Effects of a tilted magnetic field on a two-dimensional electron gas Phys. Rev. 174 823-828
- Finkelstein A M 1983 Influence of Coulomb interaction on the properties of disordered metals Sov. Phys. JETP 57 97-108
- Finkelstein A M 1984 Weak localization and Coulomb interaction in disordered-systems Z. Phys. B 56 189-196
- Fogler M M 2003 Nonlinear screening and percolative transition in a two-dimensional electron liquid P reprint cond-m at/0310010
- Gao X P A, Mills A P, Ramirez A P, Pfeiffer L N and West K W 2002 Weak-localization-like temperature-dependent conductivity of a dilute two-dimensional hole gas in a parallel magnetic field Phys. Rev. Lett. 89 016801
- Gold A and Dolgoplov V T 1986 Temperature dependence of the conductivity for the two-dimensional electron gas: Analytical results for low temperatures Phys. Rev. B 33 1076-1084
- Gold A 2001 Linear temperature dependence of mobility in quantum wells and the effects of exchange and correlation J. Phys.: Condens. Matter 13 11641-11650
- Gold A and Dolgoplov V T 2002 On the role of disorder in transport and magnetic properties of the two-dimensional electron gas J. Phys.: Condens. Matter 14 7091-7096
- Gold A 2003 Linear temperature dependence of the mobility in two-dimensional electron gases: many-body and spin-polarization effects J. Phys.: Condens. Matter 15 217-223
- Hanein Y, Meirav U, Shahar D, Li C C, Tsui D C and Shtrikman H 1998a The metallic-like conductivity of a two-dimensional hole system Phys. Rev. Lett. 80 1288-1291
- Hanein Y, Shahar D, Yoon J, Li C C, Tsui D C and Shtrikman H 1998b Properties of the apparent metal-insulator transition in two-dimensional system Phys. Rev. B 58 R7520-R7523
- Heemskerck R and Klapwijk T M 1998 Nonlinear resistivity at the metal-insulator transition in a two-dimensional electron gas Phys. Rev. B 58 R1754-R1757
- Herbut I F 2001 The effect of a parallel magnetic field on the Boltzmann conductivity and the Hall coefficient of a disordered two-dimensional Fermi liquid Phys. Rev. B 63 113102
- Hikami S, Larkin A I and Nagaoka Y 1980 Spin-orbit interaction and magnetoresistance in the two-dimensional random system Prog. Theor. Phys. 63 707-710
- Ilanis, Yacoby A, Mahalu D and Shtrikman H 2000 Unexpected behavior of the local compressibility near the  $B = 0$  metal-insulator transition Phys. Rev. Lett. 84 3133-3136
- Ilanis, Yacoby A, Mahalu D and Shtrikman H 2001 Microscopic structure of the metal-insulator transition in two dimensions Science 292 1354-1357
- Iwamoto N 1991 Static local-field corrections of 2-dimensional electron liquids Phys. Rev. B 43 2174-2182
- Jaroszynski J, Popovic D and Klapwijk T M 2002 Universal behavior of the resistance noise across the metal-insulator transition in silicon inversion layers Phys. Rev. Lett. 89 276401
- Khrapai V, Shashkin A A and Dolgoplov V T 2003 Direct measurements of the spin and the cyclotron gaps in a 2D electron system in silicon Phys. Rev. Lett. 91 126404
- Kravchenko S V, Kravchenko G V, Fumeaux J E, Pudalov V M and D'orio M 1994 Possible metal-insulator-transition at  $B = 0$  in 2 dimensions Phys. Rev. B 50 8039-8042

- Kravchenko S V, Mason W E, Bowker G E, Fumeaux J E, Pudalov V M and D'Orto M 1995 Scaling of an anomalous metal-insulator transition in a 2-dimensional system in silicon at  $B = 0$  Phys. Rev. B 51 7038-7045
- Kravchenko S V, Simonian D, Sarachik M P, Mason W and Fumeaux J E 1996 Electric field scaling at a  $B = 0$  metal-insulator transition in two dimensions Phys. Rev. Lett. 77 4938-4941
- Kravchenko S V, Simonian D, Sarachik M P, Kent A D and Pudalov V M 1998 Effect of a tilted magnetic field on the anomalous  $H = 0$  conducting phase in high-mobility Si MOSFET's Phys. Rev. B 58 3553-3556
- Kravchenko S V and Lapwijk T M 2000a Metallic low-temperature resistivity in a 2D electron system over an extended temperature range Phys. Rev. Lett. 84 2909-2912
- Kravchenko S V, Shashkin A A, Boore D A and Lapwijk T M 2000b Shubnikov-de Haas oscillations near the metal-insulator transition in a two-dimensional electron system in silicon Solid State Commun. 116 495-499
- Kravchenko S V, Shashkin A A and Dolgoplov V T 2002 Comment on "Low-density spin susceptibility and effective mass of mobile electrons in Si inversion layers" Phys. Rev. Lett. 89 219701
- Kwon Y, Ceperley D M and Martin R M 1994 Quantum Monte-Carlo calculation of the Fermi-liquid parameters in the 2-dimensional electron-gas Phys. Rev. B 50 1684-1694
- Landau L D 1957 The theory of a Fermi liquid Sov. Phys. JETP 3 920-925
- Lee P A and Ramakrishnan T V 1982 Magnetoresistance of weakly disordered electrons Phys. Rev. B 26 4009-4012
- Lee P A and Ramakrishnan T V 1985 Disordered electronic systems Rev. Mod. Phys. 57 287-337
- Lilly M P, Reno J L, Simmons J A, Spielman I B, Eisenstein J P, Pfeiffer L N, West K W, Hwang E H and Das Sarma S 2003 Resistivity of dilute 2D electrons in an undoped GaAs heterostructure Phys. Rev. Lett. 90 056806
- Mason W, Kravchenko S V, Bowker G E and Fumeaux J E 1995 Experimental evidence for a Coulomb gap in 2 dimensions Phys. Rev. B 52 7857-7859
- Mertes K M, Zheng H, Vitkalov S A, Sarachik P and Lapwijk T M 2001 Temperature dependence of the resistivity of a dilute two-dimensional electron system in high parallel magnetic field Phys. Rev. B 63 041101(R)
- Mills A P, Ramirez A P, Pfeiffer L N and West K W 1999 Nonmonotonic temperature-dependent resistance in low density 2D hole gases Phys. Rev. Lett. 83 2805-2808
- Mills A P, Ramirez A P, Gao X P A, Pfeiffer L N, West K W and Simon S H 2001 Suppression of weak localization effects in low-density metallic 2D holes Preprint cond-mat/0101020
- Noh H, Lilly M P, Tsui D C, Simmons J A, Hwang E H, Das Sarma S, Pfeiffer L N and West K W 2002 Interaction corrections to two-dimensional hole transport in the large  $r_s$  limit Phys. Rev. B 68 165308
- Okamoto T, Hosoya K, Kawaji S and Yagi A 1999 Spin degree of freedom in a two-dimensional electron liquid Phys. Rev. Lett. 82 3875-3878
- Papadakis S J and Shayegan M 1998 Apparent metallic behavior at  $B = 0$  of a two-dimensional electron system in AlAs Phys. Rev. B 57 R15068-R15071
- Papadakis S J, DePoortere E P, Shayegan M and Winkler R 2000 Anisotropic magnetoresistance of two-dimensional holes in GaAs Phys. Rev. Lett. 84 5592-5595
- Pastor A A and Dobrosavljevic V 1999 Melting of the electron glass Phys. Rev. Lett. 83 4642-4645
- Pepper M, Pollitt S and Adkins C J 1974 The spatial extent of localized state wavefunctions in silicon inversion layers J. Phys. C: Solid State Phys. 7 L273-L277
- Phillips P, Wan Y, Martin L, Knysh S and Dalidovich D 1998 Superconductivity in a two-dimensional electron gas Nature (London) 395 253-257
- Polyakov D G and Shklovskii B I 1993 Conductivity-peak broadening in the quantum Hall regime Phys. Rev. B 48 11167-11175
- Popovic D, Fowler A B and Washburn S 1997 Metal-insulator transition in two dimensions: Effects of disorder and magnetic field Phys. Rev. Lett. 79 1543-1546
- Proskuryakov Y Y, Savchenko A K, Safonov S S, Pepper M, Simmons M Y and Ritchie D A 2002 Hole-hole interaction effect in the conductance of the two-dimensional hole gas in the ballistic regime Phys. Rev. Lett. 89 076406
- Rus O, Reznikov M, Sivan U and Pudalov V M 2002 Cooling of electrons in a silicon inversion layer Phys. Rev. Lett. 88 016801
- Rus O, Yaish Y, Reznikov M, Sivan U and Pudalov V M 2003 Thermodynamic spin magnetization of strongly correlated two-dimensional electrons in a silicon inversion layer Phys. Rev. B 67 205407
- Pudalov V M, D'Orto M, Kravchenko S V and Campbell J W 1993 Zero magnetic field collective insulator phase in a dilute 2D electron system Phys. Rev. Lett. 70 1866-1869

- Pudalov V M, Brunthaler G, Prinz A and Bauer G 1997 Instability of the two-dimensional metallic phase to a parallel magnetic field JETP Lett. 65 932-937
- Pudalov V M, Brunthaler G, Prinz A and Bauer G 1998 Metal-insulator transition in two dimensions Physica E 3 79-88
- Pudalov V M, Brunthaler G, Prinz A and Bauer G 1999 Weak-field Hall resistance and effective carrier density measurements across the metal-insulator transition in Si-MOS structures JETP Lett. 70 48-53
- Pudalov V M, Brunthaler G, Prinz A and Bauer G 2001 Effect of the in-plane magnetic field on conduction of the Si-inversion layer: magnetic field driven disorder Preprint cond-mat/0103087
- Pudalov V M, Brunthaler G, Prinz A and Bauer G 2002a Weak anisotropy and disorder dependence of the in-plane magnetoresistance in high-mobility (100) Si-inversion layers Phys. Rev. Lett. 88 076401
- Pudalov V M, Gershenson M E, Kojima H, Butch N, Dizhur E M, Brunthaler G, Prinz A and Bauer G 2002b Low-density spin susceptibility and effective mass of mobile electrons in Si inversion layers Phys. Rev. Lett. 88 196404
- Pudalov V M, Gershenson M E, Kojima H, Brunthaler G, Prinz A and Bauer G 2003 Interaction effects in conductivity of Si inversion layers at intermediate temperatures Phys. Rev. Lett. 91 126403
- Punnoose A and Finkelstein A M 2002 Dilute electron gas near the metal-insulator transition: Role of valleys in silicon inversion layers Phys. Rev. Lett. 88 016802
- Rahimi A, Nissimova S, Sakr M R, Kravchenko S V and Klapwijk T M 2003 Coherent back-scattering near the two-dimensional metal-insulator transition Phys. Rev. Lett. 91 116402
- Sarachik M P and Kravchenko S V 1999 Novel phenomena in dilute electron systems in two dimensions Proc. Natl. Acad. Sci. USA 96 5900-5902
- Sarachik M P 2002 Disorder-dependence of the critical density in two-dimensional systems: An empirical relation Europhys. Lett. 57 546-549
- Sarachik M P and Vitkalov S A 2003 Does  $g$  diverge at a finite electron density in silicon inversion layers? J. Phys. Soc. Japan (Suppl. A) 72 57-62
- Senz V, Dotsch U, Gennser U, Ihn T, Heinzl T, Ensslin K, Hartmann R and Grützmacher D 1999 Metal-insulator transition in a 2-dimensional system with an easy spin axis Ann. Phys., Lpz. 8 (special issue) 237-240
- Shahar D, Tsui D C, Shayegan M, Cunningham J E, Shimshoni E and Sondhi S L 1996 Evidence for charge-ux duality near the quantum Hall liquid-to-insulator transition Science 274 589-592
- Shashkin A A, Dolgoplov V T and Kravchenko S V 1994 Insulating phases in a 2-dimensional electron-system of high-mobility Si-MOSFETs Phys. Rev. B 49 14486-14495
- Shashkin A A, Kravchenko S V, Dolgoplov V T and Klapwijk T M 2001a Indication of the ferromagnetic instability in a dilute two-dimensional electron system Phys. Rev. Lett. 87, 086801
- Shashkin A A, Kravchenko S V and Klapwijk T M 2001b Metal-insulator transition in 2D: equivalence of two approaches for determining the critical point Phys. Rev. Lett. 87, 266402
- Shashkin A A, Kravchenko S V, Dolgoplov V T and Klapwijk T M 2002 Sharp increase of the effective mass near the critical density in a metallic two-dimensional electron system Phys. Rev. B 66 073303
- Shashkin A A, Rahimi A, Nissimova S, Kravchenko S V, Dolgoplov V T and Klapwijk T M 2003a Spin-independent origin of the strongly enhanced effective mass in a dilute 2D electron system Phys. Rev. Lett. 91 046403
- Shashkin A A, Kravchenko S V, Dolgoplov V T and Klapwijk T M 2003b Sharply increasing effective mass: a precursor of a spontaneous spin polarization in a dilute two-dimensional electron system J. Phys. A: Math. Gen. 36 9237-9247
- Shashkin A A, Dolgoplov V T and Kravchenko S V 2003c Comment on "Interaction effects in conductivity of Si inversion layers at intermediate temperatures" Preprint cond-mat/0311174
- Si Q M and Varna C M 1998 Metal-insulator transition of disordered interacting electrons Phys. Rev. Lett. 81 4951-4954
- Simmons M Y, Hamilton A R, Pepper M, Linfield E H, Rose P D, Ritchie D A, Savchenko A K and Grieths T G 1998 Metal-insulator transition at  $B = 0$  in a dilute two-dimensional GaAs-AIGaAs hole gas Phys. Rev. Lett. 80 1292-1295
- Simmons M Y, Hamilton A R, Pepper M, Linfield E H, Rose P D and Ritchie D A 2000 Weak localization, hole-hole interactions, and the metal-insulator transition in two dimensions Phys. Rev. Lett. 84 2489-2492
- Simonian D, Kravchenko S V and Sarachik M P 1997a Reflection symmetry at a  $B = 0$  metal-insulator transition in two dimensions Phys. Rev. B 55 R13421-R13423
- Simonian D, Kravchenko S V, Sarachik M P and Pudalov V M 1997b Magnetic field suppression of

- the conducting phase in two dimensions Phys. Rev. Lett. 79 2304-2307
- Simonian D, Kravchenko S V, Sarachik M P and Pudalov V M 1998  $H=T$  scaling of the magnetococonductance near the conductor-insulator transition in two dimensions Phys. Rev. B 57 R9420-R9422
- Smith J L and Stiles P J 1972 Electron-electron interactions continuously variable in the range  $2.1 > r_s > 0.9$  Phys. Rev. Lett. 29 102-104
- Sondhi S L, Girvin S M, Carini J P and Shahar D 1997 Continuous quantum phase transitions Rev. Mod. Phys. 69 315-333
- Spivak B 2001 Properties of the strongly correlated two-dimensional electron gas in Si MOSFET's Phys. Rev. B 64 085317
- Spivak B 2002 Phase separation in the two-dimensional electron liquid in MOSFET's Phys. Rev. B 67 125205
- Stem F 1980 Calculated temperature dependence of mobility in silicon inversion layers Phys. Rev. Lett. 44 1469-1472
- Stoner E C 1946 Ferromagnetism Rep. Prog. Phys. 11 43-112
- Tanaskovic D, Dobrosavljevic V, Abraham S E and Kotliar G 2003 Disorder screening in strongly correlated systems Phys. Rev. Lett. 91 066603
- Tanatar B and Ceperley D M 1989 Ground-state of the two-dimensional electron-gas Phys. Rev. B 39 5005-5016
- Tutuc E, DePoortere E P, Papadakis S J and Shayegan M 2001 In-plane magnetic field-induced spin polarization and transition to insulating behavior in two-dimensional hole systems Phys. Rev. Lett. 86 2858-2861
- Tutuc E, Melinte S and Shayegan M 2002 Spin polarization and g factor of a dilute GaAs two-dimensional electron system Phys. Rev. Lett. 88 36805
- Tutuc E, Melinte S, DePoortere E P, Shayegan M and Winkel R 2003 Role of nitride layer thickness in spin polarization of GaAs two-dimensional electrons in strong parallel magnetic fields Phys. Rev. B 67 241309(R)
- Uren M J, Davies R A and Pepper M 1980 The observation of interaction and localisation effects in a two-dimensional electron gas at low temperatures J. Phys. C: Solid State Phys. 13 L985-L993
- Varna C M, Nussinov Z and van Saarloos W 2002 Singular or non-Fermi liquids Phys. Rep. 361 267-417
- Vitkalov S A, Zheng H, Mertes K M, Sarachik M P and Klapwijk Y M 2000 Small-angle Shubnikov-de Haas measurements in a 2D electron system: The effect of a strong in-plane magnetic field Phys. Rev. Lett. 85 2164-2167
- Vitkalov S A, Sarachik M P and Klapwijk T M 2001a Spin polarization of two-dimensional electrons determined from Shubnikov-de Haas oscillations as a function of angle Phys. Rev. B 64 073101
- Vitkalov S A, Zheng H, Mertes K M, Sarachik M P and Klapwijk T M 2001b Scaling of the magnetococonductivity of silicon MOSFETs: Evidence for a quantum phase transition in two dimensions Phys. Rev. Lett. 87 086401
- Vitkalov S A, Sarachik M P and Klapwijk T M 2002 Spin polarization of strongly interacting two-dimensional electrons: The role of disorder Phys. Rev. B 65 201106(R)
- Vitkalov S A, James K, Narozhny B N, Sarachik M P and Klapwijk T M 2003 In-plane magnetococonductivity of Si MOSFETs: A quantitative comparison of theory and experiment Phys. Rev. B 67 113310
- Vojsa M 2003 Quantum phase transitions Rep. Prog. Phys. 66 2069-2110
- Wigner E 1934 On the interaction of electrons in metals Phys. Rev. 46 1002-1011
- Yaish Y, Prus O, Buchstab E, Shapira S, Ben Yoseph G, Sivan U and Stem A 2000 Interband scattering and the "metallic phase" of two-dimensional holes in GaAs/AlGaAs Phys. Rev. Lett. 84 4954-4957
- Yoon J, Li C C, Shahar D, Tsui D C and Shayegan M 1999 Wigner crystallization and metal-insulator transition of two-dimensional holes in GaAs at  $B = 0$  Phys. Rev. Lett. 82 1744-1747
- Yoon J, Li C C, Shahar D, Tsui D C and Shayegan M 2000 Parallel magnetic field induced transition in transport in the dilute two-dimensional hole system in GaAs Phys. Rev. Lett. 84 4421-4424
- Zala G, Narozhny B N and Aleiner I L 2001 Interaction corrections at intermediate temperatures: Longitudinal conductivity and kinetic equation Phys. Rev. B 64 214204
- Zala G, Narozhny B N and Aleiner I L 2002 Interaction corrections at intermediate temperatures: Magnetoresistance in a parallel field Phys. Rev. B 65 020201(R)
- Zhu J, Stormer H L, Pfeiffer L N, Baldwin K W and West K W 2003 Spin susceptibility of an ultra-low-density two-dimensional electron system Phys. Rev. Lett. 90 056805